



SPEAKER PRESENTATIONS

Colored Stones and Pearls

Tourmaline: A Gemstone's Guide to Geologic Evolution of the Earth's Crust



Barbara L. Dutrow
Louisiana State University, Baton Rouge

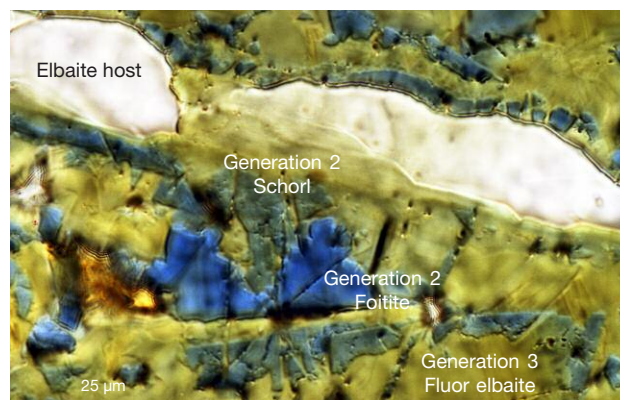
Tourmaline is recognized as an important gemstone and a stunning collector's item, and each crystal contains geochemical fingerprints that can elucidate an astonishing array of geological processes. Through field, experimental, analytical, and theoretical studies, the rich chemical signature encapsulated in tourmaline is being unraveled and revealed. Because of its widely varying chemistry, tourmaline is particularly adept at recording the host-rock environment in which it grew, be it a melt, a marble, or a former subduction zone. In addition, it can record the thermal and baric conditions of its growth, acting as a geothermometer or geobarometer. A crystal that exhibits sector zoning can provide the complete temperature history of its growth, serving as a single-mineral thermometer. Other tourmaline compositions may reveal the absolute age of a geologic event that produced tourmaline formation.

Tourmaline also excels at recording the evolution of the fluids with which it interacts. Its essential ingredient is boron (B), a fluid-mobile element. Thus, tourmaline is nature's boron recorder. Tourmaline formation and growth reflects the availability of boron to the rock system. Fluids can be sourced internally from the melt or from the breakdown of other B-bearing minerals, or fluids with boron can infiltrate the rock system from external sources. In each case, tourmaline preserves signatures of these events in the form of new growth, dissolution of preexisting tourmaline with growth of a new tourmaline composition (tourmaline cannibalizing itself to form anew), or replacement of another mineral. Tourmaline species may hint at fluid compositions. For example, species ranging from oxy-dravite to povondraite are typically found in saline, oxidizing environments and are indicators of these fluids in the geologic past. The deep green chrome (Cr) tourmalines reflect an unusual environment enriched in both Cr and B. Similarly, tourmaline compositions may reflect specific components of the fluid phase and, in some cases, provide quantitative estimates of fluid compositions (figure 1). Fitting data to tourmaline–fluid partitioning experiments permits calculation of the sodium (Na) concentrations in the coexisting fluid phase, and

suggests that the alkali species of tourmaline—elbaite, dravite, and schorl—form in fluids with greater than 0.30 mol/L Na, whereas the vacancy-dominant species, foitite and oxy-foitite, are stable in fluids with less than 0.25 mol/L Na. Once formed, tourmaline resists attack by corrosive acidic fluids.

Combining these features, tourmaline is a mineral containing unparalleled information on the environment in which it grew and the geologic processes responsible for it. An advantage of tourmaline as a geologic record keeper is that once these signals are incorporated, they are retained throughout the “lifetime” of the grain due to its slow volume diffusion. In some extraordinary cases, a single tourmaline grain can record its complete “life cycle,” from its original crystallization from a cooling magma deep within the crust through the rock's uplift, cooling, and partial destruction during erosion to

Figure 1. A single tourmaline fiber contains three distinct chemical zones, each recording the fluid composition at the time of growth. Between zones, fluids dissolved preexisting tourmaline to provide components for the new species in equilibrium. This overall compositional trend mimics the fractionation trend in a pegmatite.



deposition and reburial followed by heating and regrowth in a new geologic environment. The oldest known tourmaline dates back about 3.7 billion years, and it retains the chemical growth zones from its formation in early Earth, thus elucidating the presence of boron-bearing fluids and continental crust during that time.

The totality of this embedded geologic history is the result of tourmaline's flexible crystal structure, which incorporates a substantial number of chemical elements and isotopes, across a wide array of sizes and valence states, and in quantities from major to trace amounts. Such variable chemistry not only produces a kaleidoscope of colored gemstones but also permits tourmaline to be stable over nearly all pressure and temperature conditions found in Earth's crust, and to develop in all major rock types, from solidified igneous melts and pegmatites to metamorphic and sedimentary rocks. This chemical variability classifies tourmaline as a

mineral supergroup, currently consisting of 33 different species, each with a different and unique story.

Telling tourmaline's story typically requires chemical compositions to be obtained. New methods involving laser ablation–inductively coupled plasma–mass spectrometry (LA-ICP-MS) and infrared and Raman spectroscopy, along with well-established techniques such as electron microprobe analysis, provide such information to gemologists and geologists. For tourmaline, a mineral with one of the most exquisite arrays of color, geologists tease apart the complex clues it harbors, and gemologists can use these to tell the story of each gemstone. The widespread occurrence of the tourmaline minerals and their ability to imprint, record, and retain information make them a valuable tool for investigating Earth's geological processes. Tourmaline is the ultimate keeper of geologic information, a geologic DVD.

“Boehmite Needles” in Corundum Are Rose Channels

Franck Notari¹, Emmanuel Fritsch² (presenter), Candice Caplan¹, and Thomas Hainschwang¹

¹GGTL-Laboratories Switzerland, Geneva, and Balzers, Liechtenstein

²Institut des Matériaux Jean Rouxel and University of Nantes, France

Crystallographically oriented, linear inclusions in corundum are often referred to as “boehmite needles” or “polycrystalline boehmite” (boehmite is the orthorhombic aluminum hydroxide γ -AlOOH). These inclusions are oriented along the edges of the rhombohedral faces and form angles of about 90°. They are always found at the intersection of twin lamellae, formed by twinning along the rhombohedral faces. They contain apparently polycrystalline material tentatively identified (at least in some cases) as boehmite. These are common in natural corundum and sometimes used as a criterion to separate natural from synthetic corundum.

Boehmite can be recognized through its infrared absorption. The great majority of the “needle”-containing gem corundum showed no boehmite infrared absorption, thus leading us to believe that these inclusions have a different origin. Microscopic observation reveals three aspects: some are lath- or ribbon-shaped, others are clearly negative crystals, and sometimes

they appear as dotted lines. At the outcrop of the feature on the gem's surface there is most commonly a void that can be followed into the gem, so the “needle” is essentially empty. This feature was also documented in a flux-grown synthetic ruby with no boehmite infrared signal. These channels are favored during titanium diffusion and take on color first, as diffusion is much faster in the empty space.

It is known that in a small number of materials—some metals, calcite, and diamond—hollow channels may form at the intersection of twin lamellae, caused by deformation twinning. This was discovered by Gustav Rose (1868) in calcite, and thus the features are called “Rose channels” (figure 1). We believe that “boehmite needles” are in fact Rose channels. Even when very small, these channels would explain the optical relief observed, without a change in chemistry or infrared absorption. They fit the crystallographic nature of the structures observed.

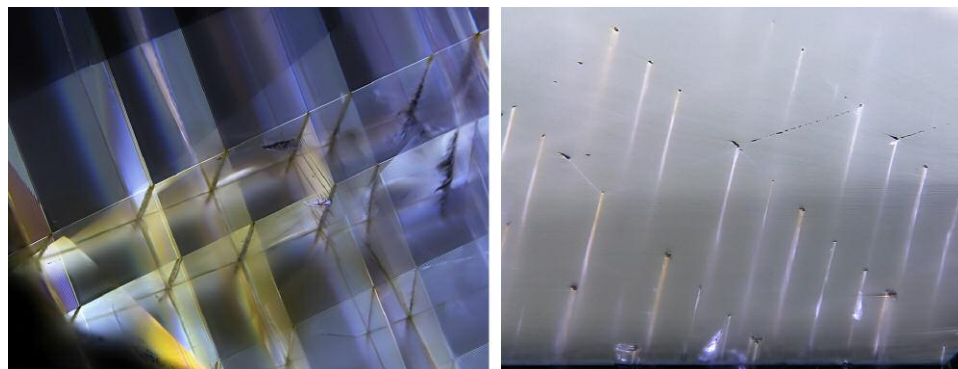


Figure 1. Left: Rose channels at the intersection of twin lamellae in a 7.17 ct color-change sapphire from East Africa, viewed in partially polarized light. Right: Detail of the same zone in reflected light, illustrating the fact that these channels are empty. Photos by Franck Notari; fields of view approximately 5.66 mm (left) and 2.83 mm (right).

Gemstones and Photoluminescence

Claudio C. Milisenda

DSEF German Gem Lab, Idar-Oberstein

Laser- and ultraviolet-excited luminescence spectroscopy and imaging are important techniques for gemstone testing, as they are among the most sensitive spectroscopic methods (see Hainschwang et al., 2013). They are able to identify optically active crystallographic defects such as vacancies and substitutions that are present in such small amounts that they cannot be detected by any other analytical method. Photoluminescence (PL) analysis became particularly important in the last decade for the separation of natural from synthetic diamonds and the detection of treatments. Today the availability of specially designed and reasonably priced portable equipment enables the rapid *in situ* identification of mounted and unmounted natural diamonds.

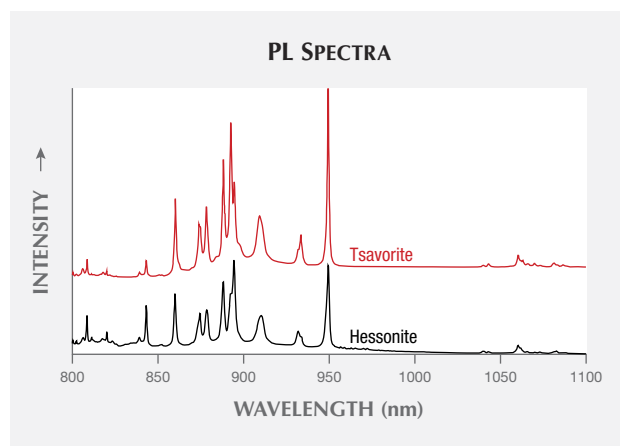
Although PL spectroscopy is most commonly used for diamond identification, it can also be applied to colored stones. Some stones exhibit unique luminescence patterns, which can be used to identify the material. Other examples are the separation of natural from synthetic spinel and the detection of heat-treated spinel. Since chromium is a typical PL-causing trace element, it is also possible to separate chromium-colored gems such as ruby and jadeite from their artificially colored counterparts. The color authenticity of specific types of corals and pearls can also be determined.

The rare earth elements (REE) are among the main substituting luminescence centers in Ca^{2+} -bearing minerals (Gaft et al., 2005). Recently, REE photoluminescence has been observed in cuprian liddicoatite tourmalines from Mozambique (Milisenda and Müller, 2017). When excited by a 785 nm laser, the stones showed a series of bands at 861, 869, 878, 894, and 1053 nm, consistent with the

PL spectra of other calcium-rich minerals (Chen and Stimets, 2014). LA-ICP-MS analysis confirmed the REE enrichment in this type of tourmaline compared to cuprian elbaïtes from Brazil and Nigeria. As a result, photoluminescence can be used as a further criterion for origin determination of Paraíba-type tourmalines.

We have extended our research on other calcium-rich gems, including various grossular garnet varieties such as hessonite and tsavorite (figure 1), uvarovite garnet, apatite, titanite, and scheelite, as well as a number of high-refractive-index glasses and color-change glasses, respectively.

Figure 1. 785 nm laser-induced REE photoluminescence spectra of tsavorite and hessonite garnets. Spectra are offset for clarity.



REFERENCES

- Chen H., Stimets R.W. (2014) Fluorescence of trivalent neodymium in various materials excited by a 785 nm laser. *American Mineralogist*, Vol. 99, No. 2-3, pp. 332–342, <https://doi.org/10.2138/am.2014.4311>
- Gaft M., Reisfeld R., Panczer G. (2005) *Modern Luminescence Spectroscopy of Minerals and Materials*. 2nd edition, Springer, Heidelberg, Germany, 606 pp.
- Hainschwang T., Karampelas S., Fritsch E., Notari F. (2013) Luminescence

spectroscopy and microscopy applied to study gem materials: a case study of C centre containing diamonds. *Mineralogy and Petrology*, Vol. 107, No. 3, pp. 393–413, <https://doi.org/10.1007/s00710-013-0273-7>

Milisenda C.C., Müller S. (2017) REE photoluminescence in Paraíba type tourmaline from Mozambique. *35th International Gemmological Conference*, Windhoek, Namibia, pp. 71–73.

An Overview of Asteriated Gems: From Common Star Sapphire to Rare Star Aquamarine to One-of-a-Kind Star Zircon

Martin P. Steinbach

Steinbach-Gems with a Star, Idar-Oberstein, Germany

Rays of angel's hair in a star-like shape, beams of light hovering over the surface of a gem—gems with stars have fascinated people of all cultures, continents, and religions since ancient times.

Asteriated gems have been known for more than 2,000 years, starting with Periegetes' description of "Asterios" in the first century BCE. Other historical names were *asteria*, *asterius*, *astrion*,

astrodamas, and *astriotes*. From Pliny the Elder (first century CE) to the Middle Ages, to De Boodt (1609) and Brueckmann (1783), asterism was known only in corundum and some feldspar varieties.

Currently, about 60 different gem varieties display asterism, whereas 15 gemstone varieties show a “trapiche” star. The well-known commercial examples include star ruby, sapphire, quartz, almandine garnet, moonstone (orthoclase feldspar), and the four-rayed black star diopside from India. Rare or less well-known varieties include star aquamarine, beryl, bronzite, calcite, chrysoberyl (A.G.S. Research Service, 1937), enstatite, hypersthene, kyanite, peridot, scheelite, scapolite, spinel, and sunstone (oligoclase feldspar). The extremely rare one-of-a-kind stars consist of star alexandrite, amazonite (Steinbach, 2016), cordierite, apatite, “star diamond,” ekanite, emerald (Liddicoat, 1977), kornerupine, kunzite, labradorite, opal, parisite, prehnite, rhodochrosite (figure 1), rhodonite, rutile, serandite, fibrolite (sillimanite), spessartine, taaffeite, tanzanite, topaz, tourmaline, and zircon.

Some of the 60 different star stones introduced in this colorful presentation can also show double stars; 12-, 18-, or 24-rayed stars; a network of stars; and trapiche varieties.

REFERENCES

A.G.S. Research Service (1937) Star chrysoberyl. *G&G*, Vol. 2, No. 8, p. 130.
Liddicoat R.T. (1977) Comments on the Hixon Collection. *G&G*, Vol. 15, No. 9, p. 1.



Figure 1. This 15.51 ct star rhodochrosite is from the Sweet Home mine in the state of Colorado. Photo by Martin P. Steinbach.

One new source of star rose quartz (China) and two new sources of almandine star garnet (China and Russia) will also be presented.

Steinbach M.P. (2016) *Asterism—Gems with a Star*. MPS Publishing and Media, Idar-Oberstein, Germany, 896 pp.

Quantitative Identification of Green Nephrite from Five Major Origins In Asia and North America

Zemin Luo, Andy H. Shen, and Meihua Chen
China University of Geosciences, Wuhan

Green nephrite (serpentine-related) has been generating substantial interest in the gem market. The primary sources are China, Russia, and Canada. Preliminary observations of mineral impurities and chemical components can help separate some dolomite-related nephrite from serpentine-related material. We have developed a novel classifier that can automatically identify the geological origin of random green nephrite samples on the market with 95% prediction accuracy. The technique behind this classi-

fier is based on a trace-element database for green nephrite and a machine learning algorithm.

The green nephrite database was built from 34 samples from five major geological origins (Manasi and Hetian in Xinjiang, China; Taiwan; British Columbia, Canada; and Siberia, Russia; representative samples are shown in figure 1). Trace-element information was collected by LA-ICP-MS with an average of six points on each sample. The following classification models were

Figure 1. Representative green nephrite samples from the five serpentine-related deposits in Asia and North America: Manasi (A), Hetian (B), Taiwan (C), British Columbia (D), and Siberia (E).



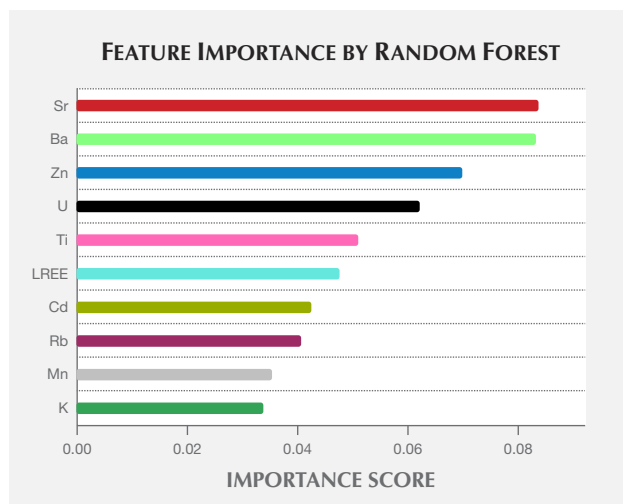


Figure 2. The 10 most important trace elements for green nephrite classification, ranked in descending order, analyzed by the random forest algorithm.

tested: neural network (multilayer perceptron), random forest, logistic regression, naive Bayes, and support vector machine. The random forest model gives the best performance on both training sets and cross-validation sets, with over 90% accuracy (table 1). The random forest model also identified the 10 most important trace elements for green nephrite classification as Sr, Ba, Zn, U, Ti, LREE, Cd, Rb, Mn, and K (figure 2). The geological information about this trace-element “fingerprint” needs further investigation.

We used linear discriminant analysis (LDA) to visually demonstrate the obvious separation of Siberian and Manasi green nephrites from the other origins (figure 3). This result is consistent with our optic and spectra characterization results. Green nephrite from the Manasi mine usually presents a heterogeneous grayish yellow green color, which is quite different from that of other origins. The absence of garnet inclusions in Siberian green nephrite—which distinguishes it from material from the other localities—can be confirmed by Raman spectroscopy. Samples from all origins have been characterized by photomicrography, micro-infrared spectra, and Raman spectra. We can therefore integrate the spectra

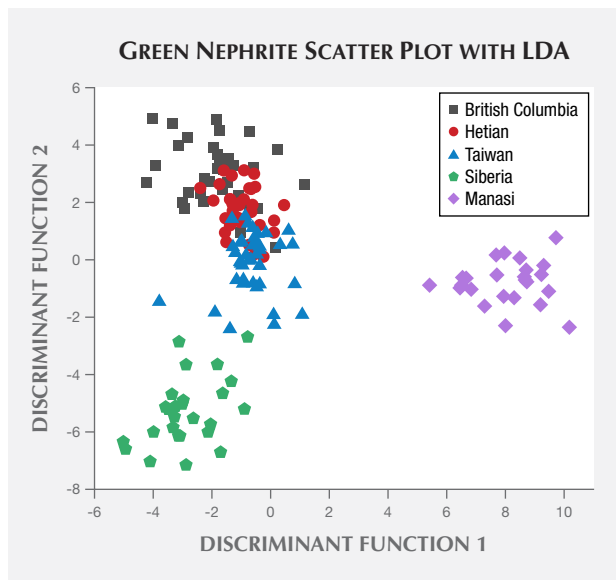


Figure 3. This scatter plot illustrates how an LDA algorithm was used to separate green nephrite. It shows clear separation of Manasi and Siberian nephrite from the other three origins (Hetian, British Columbia, and Taiwan), which show obvious overlap.

TABLE 1. Classification accuracies (%) of the training set and the cross-validation set for the five green nephrite samples using various machine learning algorithms.

Model	Score_train	Score_CV
Random forest	100.0	95.4
Neural network	99.8	92.2
Support vector machine	100.0	85.8
Logistic regression	95.3	83.2
Naive Bayes	88.2	82.6

and trace-element features into our classification model in the next step. We believe that the research method proved in this work is also applicable for other gemstones. It can also be a useful tool to study ancient green nephrite origins.

Radiocarbon Measurements on Pearls: Principles, Complexities, and Possibilities

Gregory Hodgins

University of Arizona Accelerator Mass Spectrometry Laboratory, Tucson

Radiocarbon dating is a method for determining the age of organic remains formed in the past 45,000 years. Also known as carbon-14 or ^{14}C (figure 1), radiocarbon is a naturally occurring radioactive isotope of carbon with a half-life of 5,730 years. It is continuously formed in the earth’s upper atmosphere and makes

its way into the biosphere via photosynthetic uptake and the food chain. Several radiocarbon dates for pearls have recently appeared in the scientific literature. Mollusks take up radiocarbon during life and incorporate it into shell and pearl carbonate. The aim of this presentation will be to describe the method, identification

complexities, and challenges inherent in dating pearls based upon radiocarbon measurement so that we may plot a path for future research.

There are two variants of the dating method. The first is conventional radiocarbon dating, which applies to organisms that lived before 1955 CE. The second involves the detection of anthropogenic radiocarbon in organisms living between 1955 CE and the present. There are biological, environmental, and experimental complexities in the radiocarbon dating of pearls, and the method will not work in all circumstances. However, some of these complexities—coupled with historic changes in when, where, and how pearls have been produced—mean radiocarbon measurement can provide information unavailable by other means.



Figure 1. The author stands beside the terminus of the accelerator mass spectrometer radiocarbon beam line. Photo by Gretchen Gibbs.

Unconventional Techniques in Pearl Testing: Their Potential and Limitations

Chunhui Zhou
GIA, New York

Current routine pearl testing involves the application of various basic and advanced gemological techniques. These include the use of the gemological microscope, ultraviolet (UV) luminescence, microradiography, computed X-ray microtomography, optical X-ray luminescence, energy-dispersive X-ray fluorescence spectrometry (EDXRF), ultraviolet-visible (UV-Vis) spectroscopy, and Raman spectroscopy. While the majority of pearls may be identified using these existing conventional techniques, in certain cases identification challenges remain.

This talk will discuss the potential and limitations of various unconventional techniques that have been applied to pearl testing over recent years. Some of these techniques have been explored by GIA and resulted in meaningful benefits to the trade, and others referenced in the literature will also be briefly covered. Examples of these techniques include radiocarbon age dating, deoxyribonucleic acid (DNA) bar coding, in-depth trace-element geochemistry and isotope analysis, and 3D reconstruction of internal structures. It is important for gemological and research institutions to continue developing novel techniques for pearl testing in order to achieve the accurate separation between natural and cultured pearls, principally non-bead cultured, as well as other aspects of identification that

might assist in reaching this accurate analysis (e.g., species determination, geographical origin determination, and treatment identification). Despite decades of pearl testing experience, some challenges remain within laboratories, and the application of additional unconventional methods could resolve some of these issues.

Figure 1. The application of unconventional pearl testing methods could be useful in separating difficult pearl samples, such as various types of freshwater pearls shown here. Photo by Diego Sanchez.



ADDITIONAL READING

- Krzemnicki M.S., Hajdas I. (2013) Age determination of pearls: A new approach for pearl testing and identification. *Radiocarbon*, Vol. 55, No. 3, pp. 1801–1809, <http://dx.doi.org/10.1017/S0033822200048700>
- Meyer J.B., Cartier L.E., Pinto-Figueroa E.A., Krzemnicki M.S., Hänni H.A., McDonald B.A. (2013) DNA fingerprinting of pearls to determine their origins. *PLOS One*, Vol. 8, No. 10, pp. 1–11, <http://dx.doi.org/10.1371/journal.pone.0075606>
- Saruwatari K., Suzuki M., Zhou C., Kessrapong P., Sturman N. (2018) DNA

techniques applied to the identification of *Pinctada fucata* pearls from Uwajima, Ehime Prefecture, Japan. *G&G*, Vol. 54, No. 1, pp. 40–50, <http://dx.doi.org/10.5741/GEMS.54.1.40>

- Zhou C., Hodgins G., Lange T., Saruwatari K., Sturman N., Kiefert L., Schollenbruch K. (2017) Saltwater pearls from the pre- to early Columbian era: A gemological and radiocarbon dating study. *G&G*, Vol. 53, No. 3, pp. 286–295, <http://dx.doi.org/10.5741/GEMS.53.3.286>

What Is Cobalt Spinel? Unraveling the Causes of Color in Blue Spinel

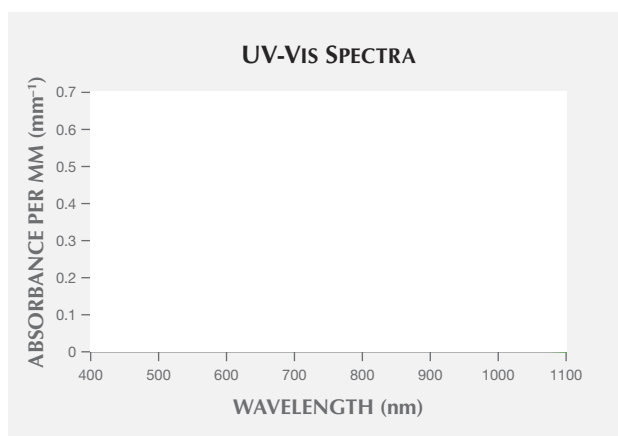
Aaron C. Palke and Ziyin Sun
GIA, Carlsbad, California

Cobalt is known to produce vibrant blue color in both natural and synthetic spinel. In the 1980s and '90s, Vietnam started producing blue spinel with very high concentrations of cobalt and bright, saturated color rivaling that seen in synthetic material. Iron can also cause blue coloration in spinel, although this is typically a duller grayish or greenish blue. So when is a blue spinel worthy of carrying the “cobalt spinel” moniker? With high-sensitivity analytical methods such as LA-ICP-MS, cobalt can be detected in most spinel, even at the sub-ppm level. But sub-ppm concentrations of cobalt do not impact the color of a faceted spinel. In addition, the saturation and quality of blue color will depend on the concentration of iron and its valence state (e.g., Fe^{2+} vs. Fe^{3+}).

In this contribution we will explore the color space of blue spinel and outline the various contributions to their coloration. Using UV-Vis spectrometry and LA-ICP-MS on blue spinel from Vietnam, Sri Lanka, Madagascar, and Tanzania, we have isolated three unique and consistent chromophores (see figure 1). Cobalt in its divalent form (Co^{2+}) has multiple absorption bands between ~510 and 660 nm and produces a bright blue color. Two broad absorption bands at ~650 and 920 nm are related to Fe^{2+} substituting for Al^{3+} in octahedral coordination. Finally, another set of at least three absorption bands occurs at ~500–620 nm and overlaps those from Co^{2+} . Comparison with other Fe-related absorption bands and consideration of the crystal chemistry of spinel suggest that these bands may be related to Fe^{3+} in the tetrahedral site in the spinel structure. This last absorption feature creates a grayish pink coloration, and in combination with Co^{2+} it can be

responsible for blue to violet color change in some spinel. There is clearly a significant interplay between these three chromophores, and a full understanding of the causes of color in blue spinel can only be attained by consideration of all three contributions.

Figure 1. UV-Vis spectra of the individual contributions from three chromophores in blue spinel, octahedral ferrous iron (Fe^{2+}), octahedral cobalt (Co^{2+}), and tetrahedral ferric iron (Fe^{3+}). At the top is the full spectrum of a blue spinel from Tanzania, followed by the sum of the three individual components (SUM). UV-Vis spectra of all blue spinels in this study could be recreated with varying contributions from the three spectra at the bottom.



Diamond Identification

Canary Yellow Diamonds

Wuyi Wang¹ and Terry Poon²

¹GIA, New York

²GIA, Hong Kong

Isolated nitrogen is one of the major defects in producing yellow color in natural diamonds. In regular type Ib yellow diamonds, isolated nitrogen is normally the dominant form, with limited aggregations in A centers (nitrogen pairs). Type Ib diamonds normally experienced strong plastic deformations. In addition to vacancy clusters, many other optic centers were introduced during annealing over their long geological history, such as GRI, NV, and H3 centers. Diamonds from the Zimmi area of West Africa are a

typical example (Smit et al., 2016). As a result, clear brownish and greenish hues are common among these diamonds, so most do not possess true “canary” yellow color. Here we studied more than 2,000 diamonds with real canary yellow color. Their color origin and relationship with type Ib diamonds were explored.

Sizes of the studied diamonds ranged from 0.01 to about 1.0 ct. They showed pure yellow color, with grades of Fancy Intense or Fancy Vivid yellow. Infrared absorption analysis showed that



they were all type IaA with very high nitrogen concentrations, but a very weak absorption from isolated nitrogen at 1344 cm^{-1} was detected in all samples. Concentration of isolated nitrogen was estimated at $\sim 2\text{--}3$ ppm. This isolated nitrogen created smooth absorption in the ultraviolet-visible (UV-Vis) region, increasing gradually to the high-energy side. No other defects were detected using UV-Vis absorption spectroscopy, which explained the pure yellow color we observed. Fluorescence imaging revealed multiple nucleation centers with dominant green color, which was attributed to the S3 defects confirmed through photoluminescence analysis. Compared with natural type Ib diamonds, an outstanding feature of the studied samples is the absence of plastic deformation. For this reason, other vacancy-related defects were not introduced to these diamond lattices over the geological period after their formation.

Sulfide inclusions are common in type Ib diamonds, but they were not observed in these canary stones. Instead, some calcite inclusions were observed. All the observations from this study indicated that the canary diamond samples were formed in a different geological environment than type Ib diamonds.

REFERENCE

Smit K.V., Shirey S.B., Wang W. (2016) Type Ib diamond formation and preservation in the West African lithospheric mantle: Re-Os age constraints from

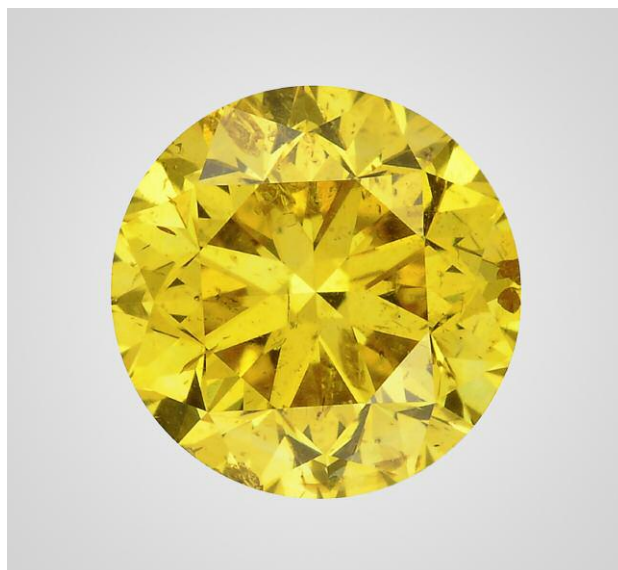


Figure 1. The canary yellow diamonds from this study showed much lower concentrations of isolated nitrogen than regular type Ib yellow diamonds, which usually show brownish and greenish hues linked to plastic deformation. Photo by Sood Oil (Judy) Chia.

sulphide inclusions in Zimmi diamonds. *Precambrian Research*, Vol. 286, pp. 152–166, <http://dx.doi.org/10.1016/j.precamres.2016.09.022>

Addressing the Challenges of Detecting Synthetic Diamonds

David Fisher

De Beers Technologies, Maidenhead, United Kingdom

The dream of growing synthetic diamonds existed for many centuries before it was achieved in the 1950s. The development of techniques to identify synthetic diamonds and enable their reliable separation from natural diamonds has not had the luxury of centuries to work with. Since the early reports on the characteristics of laboratory-grown stones, scientists have been working steadily to establish and improve the means of detection. For many years the De Beers Group has been developing equipment for rapidly screening and testing for potential synthetic and treated diamonds as part of a strategy aimed at maintaining consumer confidence in natural untreated diamonds. This work has been underpinned by extensive research into defects in natural and synthetic diamond, either conducted within De Beers' own facilities or through financial and practical support of research in external institutions.

Key to any detection technique for synthetic diamonds is a fundamental understanding of the differences between them and natural diamonds. This could take the form of differences in the atomic impurity centers or differences in the spatial distributions of these centers brought about by very significant distinctions in the growth

environments. The former was used in the development of the DiamondSure instrument that, among other things, detects variance differences in the absorption spectra due to the presence or absence of the N3 feature. This absorption is from a nitrogen-related defect that is usually only produced in nitrogen-containing diamonds by extended periods at relatively high temperatures—that is, conditions generally experienced by natural diamonds. Growth-related differences in impurity distributions can be very accurately imaged using the DiamondView instrument. Short-wave ultraviolet (UV) light is used to excite luminescence from a very thin layer of diamond near the surface to give images free from the blurring encountered with more common longer-wavelength excitation sources. DiamondView has, since its launch, provided the benchmark for the detection of synthetic diamonds.

A number of approaches involving absorption features have been developed, including the use of almost complete absorption in the ultraviolet region of the spectrum to indicate that a diamond is not synthetic. The UV absorption is produced by the A center (two adjacent nitrogen atoms) and is rarely encountered in as-

grown synthetic diamonds. The main form of nitrogen in synthetic diamonds is a single substitutional nitrogen atom that absorbs in both the ultraviolet and visible regions to produce yellow color. The combination of UV absorption and no strong yellow color is therefore restricted to natural diamond. However, treatment of nitrogen-containing synthetic diamonds is capable of generating A centers, but generally does not produce a colorless stone. This effect accounts for the careful color ranges often applied to instruments relying on UV absorption for screening. This also highlights one of the limitations of absorption spectroscopy: When smaller stones are tested, the amount of absorption decreases and the technique becomes less reliable. In recent years we have seen a shift to smaller sizes (below 0.01 ct) in the synthetic diamonds being offered for sale to the jewelry market, and screening techniques have had to evolve to address this situation and the limitations of absorption-based approaches.

Testing melee-sized diamonds, as well as introducing technical challenges around the measurement technique, has also led to the introduction of greater automation. In 2014 the De Beers Group introduced the first automated melee screening instrument (AMS1), which combined the measurement technique from DiamondSure with automated feeding and dispensing of stones in the range of 0.20 to 0.01 ct. While this instrument was well received and effectively addressed concerns around synthetic melee-sized stones in the trade at the time, there soon came calls for improvements—a faster instrument capable of measuring smaller stones, no restrictions on cut, and a lower referral rate for natural diamonds. These requirements proved impossible to meet with the limitations imposed by absorption measurements, and a new technique based on time-resolved spectroscopy was developed. This resulted in the AMS2 instrument, launched in March 2017. The AMS2 processes stones at a speed of one stone per second, 10 times faster than the AMS1. It measures round brilliants down to 0.003 ct (0.9 mm diameter) and can be used on other cuts for stones of 0.01 ct and above. The measurement technique itself has been incorporated into the SYNTHdetect (figure 1, left), an instrument launched in September 2017 that allows manual observation of the time-resolved emission. Besides providing the same testing capability as AMS2 (figure 1, right) for loose stones, various holders allow testing of mounted stones in a wide range of configurations. The benefit of this approach is that stones tested loose using AMS2 will generate a broadly consistent result when mounted on SYNTHdetect.

Changes in growth processes for synthetic diamonds have also led to the gradual introduction of new characteristics. High-pressure, high-temperature (HPHT) synthetics have tended to be fairly consistent in their growth-related luminescence patterns, while significant variations in the features associated with chemical vapor deposition (CVD) synthetics have been observed. These continue to be well documented and have led to the gradual evolution of the DiamondView instrument and the way in which it is used.



Figure 1. The De Beers Group instruments SYNTHdetect (left) and AMS2 (right) provide screening capability for melee-size diamonds as small as 0.3 points. Photo courtesy of Danny Bowler © De Beers Group.

Post-growth treatment of synthetic diamonds can be applied for a number of reasons: improvement in the color, modification of the atomic defects to make the stones look more like a natural diamond, and removal of a characteristic that could be used to identify a synthetic diamond. The motivation for the latter two treatments can only be described as fraudulent. The challenge in developing detection instruments and techniques is to ensure that they are as robust as possible in the face of such challenges. Treatment techniques will rarely have any effect on the growth patterns associated with synthetic diamonds, and it is therefore very difficult to treat synthetics in a way that would make them undetectable using the DiamondView. Screening instruments tend to be based on a single technique, and it is important that the approach adopted not be vulnerable to simpler forms of treatment. This has been of primary concern to the De Beers Group in the development of our own screening instruments. It has also been necessary in certain cases to withhold detailed information about detection techniques where disclosure of this would lead to undermining of the detection technique itself.

The De Beers Group continues to invest heavily in growth and treatment research in order to develop the next generation of instruments and techniques that will assist the trade in maintaining detection capability to support consumer confidence. The Group is uniquely placed in the industry to address these challenges due to its collaboration with Element Six (world leaders in synthesis of diamond for industrial and technical applications) and its in-depth knowledge of the properties of natural diamonds with known provenance from its own mines.

Diamond at the Diffraction Limit: Optical Characterization of Synthetic Diamond

Phil L. Diggle^{1,2}, Ulrika F.S. D'Haenens-Johansson³, Wuyi Wang³, and Mark E. Newton^{1,2}

¹Department of Physics, University of Warwick, Coventry, United Kingdom

²EPSRC Centre for Doctoral Training in Diamond Science and Technology, Warwick, United Kingdom

³GIA, New York

Diamond, known for its splendor in exquisite jewelry, has been synthesized since the 1950s. In the last six decades, the perfection of laboratory-grown single-crystal diamond has vastly improved through the research and development of two main synthesis techniques. One replicates Earth's natural process, where the diamond is grown in the laboratory under conditions of diamond stability at high temperature and high pressure (HPHT). The other technique relies on the dissociation of methane (or other carbon-containing source gas) and hydrogen and the subsequent deposition of diamond at low pressures from the gaseous phase in a process known as chemical vapor deposition (CVD). In the latter case, diamond is not the stable form of carbon, but the kinetics in the CVD process are such that diamond wins out. Large gem-quality synthetic diamonds are now possible, and a 6 ct CVD (2018) and a 15.32 ct HPHT (2018) have been reported.

It is of course possible to differentiate laboratory-grown from natural diamond based on how extended and point defects are incorporated into the crystal. Furthermore, treated diamond can be identified utilizing knowledge of how defects are produced and how they migrate and aggregate in both natural and synthetic diamond samples. Room-temperature confocal photoluminescence microscopy can be used to image the emission of light from defects in diamond with a spatial resolution limited only by the diffraction limit; a lateral spatial resolution approaching 300 nm is routinely achieved (figure 1). It is possible with this tool to identify point defects with concentrations less than 1 part per trillion (10^{11} cm^{-3}).

This talk will outline the experimental setup, how this tool has been used to identify the decoration of dislocations with point defects in CVD lab-grown diamond, and how different mechanisms for defect incorporation operate at growth sector boundaries in HPHT synthetic diamond.

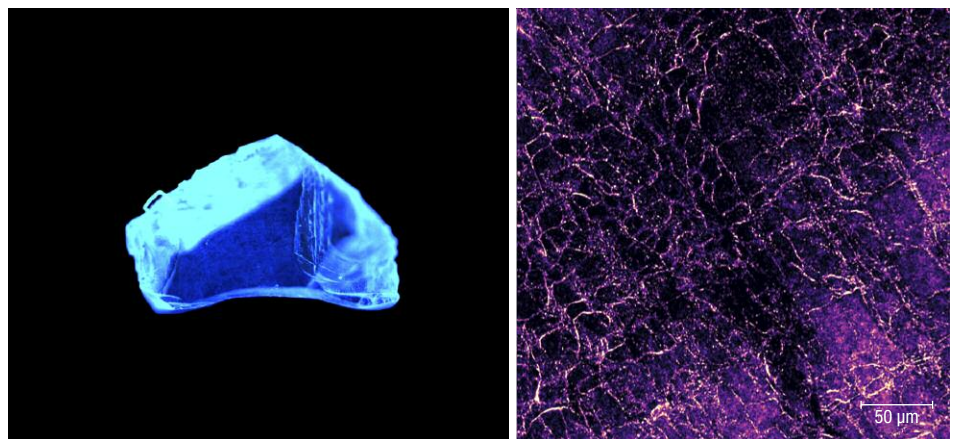


Figure 1. Left: DiamondView fluorescence imaging shows dislocation networks in a natural type IIa diamond. Right: A room-temperature confocal photoluminescence image taken with 488 nm excitation shows H3 defects following a dislocation network pattern within the diamond. Some of the fluorescent spots are single H3 centers.

Fluorescence in Diamond: New Insights

Ans Anthonis, John Chapman, Stefan Smans, Marleen Bouman, and Katrien De Corte
HRD Antwerp, Belgium

The effect of fluorescence on the appearance of diamonds has been a subject of debate for many years (Moses et al., 1997). In the trade, fluorescence is generally perceived as an undesirable characteristic. Nearly 80% of diamonds graded at HRD Antwerp receive a “nil” fluorescence grade, while the remainder are graded

as “slight,” “medium,” and “strong,” their value decreasing with level of fluorescence.

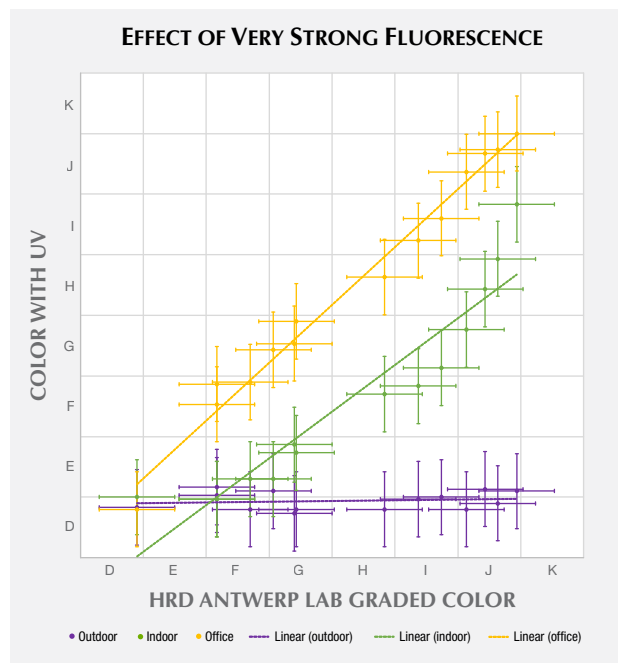
To understand how fluorescence might change diamond appearance, a selection of 160 round brilliant-cut diamonds were investigated in detail. This study focused on the effect of

fluorescence on diamond color. The aim was to determine under what lighting conditions the color of a diamond could change and the magnitude of that effect. We also investigated a smaller selection of diamonds with multiple spectroscopic absorption techniques to study the origin of their fluorescence.

The lighting arrangement we used combined the UV from light-emitting diode (LED) lamps with the light from a daylight-equivalent (grading) fluorescent lamp that had its UV component filtered out. With controlled UV output and after calibrations, it was possible to simulate different illuminations, including outdoors, indoors near a window, office lighting, and grading environments. The grading environment provided the reference color. Diamonds were presented in both table-down and table-up orientations, with the degree of effect determined by visual comparison with nonfluorescent master stones. For each color, both experienced diamond graders and nonprofessionals examined the possible effect of fluorescence on color appearance.

It was found that the UV level in office lighting was insignificant and did not produce any observable effect even with “very strong” fluorescence. However, with daylight from either outdoors or indoors, near a window, the relative strength of UV was significant, sufficient to create a positive color change. For samples with a “very strong” fluorescence, the results are shown in figure 1. For each color, ranging from D to J, the color shift caused by exposure to different UV levels—represented by the different lighting conditions—is illustrated.

Figure 1. For samples with “very strong” fluorescence, the observed color in different lighting conditions (outdoor, indoor, and office) is shown. These samples were graded through the pavilion (table-down). Note that in an outdoor environment, J colors can appear as D colors.



REFERENCE

Moses T.M., Reinitz I.M., Johnson M.L., King J.M., Shigley J.E. (1997) A contribution to understanding the effect of blue fluorescence on the appearance

of diamonds. *G&G*, Vol. 33, No. 4, pp. 244–259, <http://dx.doi.org/10.5741/GEMS.33.4.244>

Fluorescence, Phosphorescence, Thermoluminescence, and Charge Transfer in Synthetic Diamond

Jiahui (Gloria) Zhao^{1,2}, B.G. Breeze^{1,3}, B.L. Green¹, Phil L. Diggle^{1,2}, and Mark E. Newton^{1,2}

¹Department of Physics, University of Warwick, Coventry, United Kingdom

²EPSRC Centre for Doctoral Training in Diamond Science and Technology, Warwick, United Kingdom

³Spectroscopy Research Technology Platform, University of Warwick, Coventry, United Kingdom

Photoluminescence (PL) and phosphorescence underpin many of the discrimination techniques used to separate natural from synthetic diamond. PL is at the heart of many new quantum technologies based on color centers in lab-grown diamonds. In HPHT synthetic diamond, the phosphorescence observed is explained in terms of donor-acceptor pair recombination. The thermal activation of electrons to neutral boron acceptors shows that boron plays a key role in the phosphorescence process. However, there are a number

of things we struggle to explain. For example, the phosphorescence peak positions are not fully explained, and there is no conclusive link between the emission and charge transfer involving the substitutional nitrogen donor.

Secondly, the origin of the phosphorescence observed in some synthetic diamond samples grown by the CVD process is unclear. Although we now have evidence for unintentional boron impurity incorporation at stop-start growth boundaries in some CVD syn-

thetic samples, it is possible that some of the observed phosphorescence does not involve boron impurities.

In this paper we report on the results of combined fluorescence, phosphorescence, thermoluminescence, and quantitative

charge transfer investigations undertaken on both HPHT and CVD synthetic diamond, with the objective of identifying which defects are involved in the fluorescence and phosphorescence processes.

LPHT-Treated Pink CVD Synthetic Diamond

Hiroshi Kitawaki, Kentaro Emori, Mio Hisanaga, Masahiro Yamamoto, and Makoto Okano
Central Gem Laboratory, Tokyo

Pink diamond is extremely popular among fancy-color diamonds, which has prompted numerous attempts to produce pink diamond artificially. Pink CVD synthetic diamonds appeared on the gem market around 2010. Their color was produced by a multi-step process combining post-growth HPHT treatment to remove the brown hue and subsequent electron irradiation, followed by low-temperature annealing. Pink CVD synthetic diamonds treated only with low pressure and high temperature (LPHT), without additional post-growth irradiation, have also been reported but are rarely seen on the market.

Recently, a loose pink stone (figure 1) was submitted to the Central Gem Laboratory in Tokyo for grading purposes. Our examination revealed that this 0.192 ct brilliant-cut marquise was a CVD synthetic diamond that had been LPHT treated.

Visually, this diamond could not be distinguished from natural diamonds with similar color. However, three characteristics of CVD origin were detected:

1. C-H related absorption peaks between 3200 and 2800 cm^{-1} , located with infrared spectroscopy
2. A luminescence peak at 737 nm, detected with photoluminescence (PL) spectroscopy
3. A trace of lamellar pattern seen in the DiamondView

However, irradiation-related peaks such as at 1450 cm^{-1} (H1a), 741.1 nm (GR1), 594.3 nm, or 393.5 nm (ND1) that are seen in the pink CVD diamonds treated with common multi-step processes were not detected.

The presence of four peaks at 3123, 2901, 2870, and 2812 cm^{-1} between 3200 and 2800 cm^{-1} suggests this stone was LPHT treated; the following observations indicate that it was not HPHT treated:

- The 3123 cm^{-1} peak presumably derived from NVH⁰ disappears after a normal HPHT treatment.
- The 2901, 2870, and 2812 cm^{-1} peaks are known to shift toward higher wavenumbers as the annealing temperature rises. Our own HPHT treatment experiments on CVD-grown diamonds proved that the 2902 and 2871 cm^{-1} peaks detected after 1600°C annealing shifted to 2907 and 2873 cm^{-1} after 2300°C annealing. The peak shift of 2901,

2870, and 2812 cm^{-1} is also related to the pressure during the annealing, as these peaks shifted to 2902, 2871, and 2819 cm^{-1} at the higher pressure of 7 GPa compared to 2900, 2868, and 2813 cm^{-1} at the ambient pressure under the same annealing temperature of 1600°C.

- Absorption peaks at 7917 and 7804 cm^{-1} in the infrared region and at 667 and 684 nm in the visible range were also detected, which coincide with the features seen in LPHT-treated stones. From the combination of the intensity ratios of optical centers such as H3 and NV centers that were detected with PL measurement, this sample is presumed to have been treated with LPHT annealing at about 1500–1700°C as a post-growth process.

In recent years, CVD synthetic diamonds have been produced in a wider range of colors due to progress in the crystal growth techniques and post-growth treatments. Although HPHT treatment has been employed mainly to improve the color in a diamond, LPHT annealing may become widespread as the technique is further developed. Gemologists need to have deep knowledge about the optical defects in such LPHT-treated specimens.

Figure 1. LPHT-treated brownish pink CVD synthetic diamond weighing 0.192 ct. Photo by Hiroshi Kitawaki.



Recent Developments in Detection and Gemology in China, Particularly for Chinese Synthetic Diamonds

Jie Ke, Taijin Lu (presenter), Yan Lan, Zhonghua Song, Shi Tang, Jian Zhang, and Hua Chen
National Gemstone Testing Center (NGTC), Beijing

China is the world's largest producer of HPHT-grown industrial diamonds. Its 2016 production of about 20 billion carats accounted for 98% of the global supply. Since the beginning of 2015, melee-sized colorless HPHT synthetic diamonds have been tested at the National Gemstone Testing Center's (NGTC) Shenzhen and Beijing laboratories in parcels submitted by different clients, which means that colorless HPHT synthetic diamonds have entered the Chinese jewelry market and may be mistaken for natural diamonds.

CVD synthesis technology has grown rapidly in recent years. Large colorless and colored (blue, pink) CVD-grown diamonds have been entering the market, and a few have been fraudulently sold as natural diamonds.

China has independently developed gem-grade HPHT synthetic diamond production technology since 2002, and can grow gem-grade type Ib, IIa, and IIb and high-nitrogen-content synthetic diamonds in volume, depending on market needs. Gem-grade type Ib, IIa, and IIb HPHT synthetic diamonds have been grown using the temperature gradient method, under a cubic press at high pressure (e.g., 5.4 GPa) and high temperature

Figure 1. DiamondView fluorescence image of the hybrid natural and CVD-grown diamond. Photo by Shi Tang.

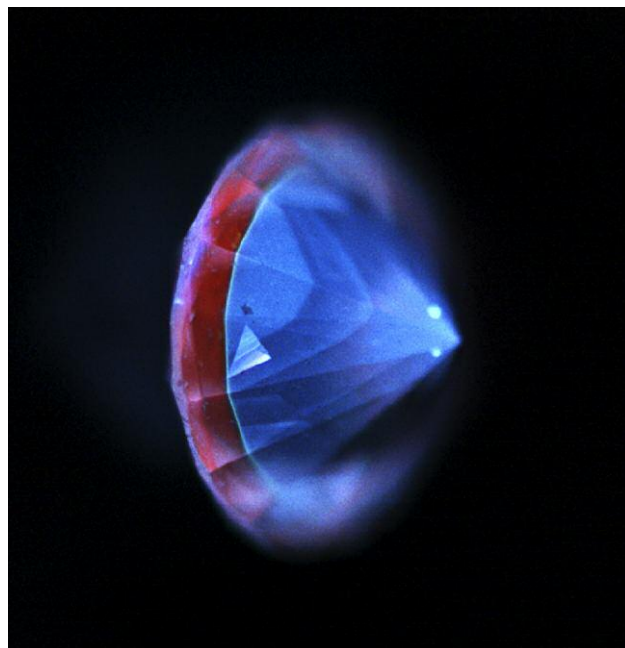


TABLE 1. Technology and products of some Chinese CVD synthetic diamond companies.

Company	Ningbo Crysdiem Industrial Technology	Hebei Plasma Diamond Technology	Shanghai Zhengshi Technology
Products and quality	Crystal size: 9 × 9 × 4 mm. Mass production of diamonds larger than 1 ct; type IIa and IIb; colorless to near-colorless, pink, and blue.	Crystal size: 11 × 11 × 1–3 mm. Scientific research, industrial production.	Crystal size: 12 × 12 × 3 mm, mainly 1.0–6.0 ct. Mass production available. Type IIa and IIb.
Growth technology	Microwave plasma chemical vapor deposition (MPCVD)	DC arc plasma jet CVD	MPCVD

(1300–1600°C). Driven by a specific temperature gradient, the carbon source from high-purity graphite (>99.9%) located at the high-temperature zone can diffuse into the seed crystals in the cubic press, resulting in the crystallization of synthetic diamonds. Chinese production of melee-sized colorless to near-colorless HPHT synthetic diamonds accounts for about 90% of the global output.

Gem-grade type IIa and IIb CVD synthetic diamonds are grown using the microwave plasma chemical vapor deposition (MPCVD) and direct current (DC) arc plasma methods. Faceted colorless CVD diamonds can be grown in sizes up to 6 ct by at least two Chinese companies (table 1).

After testing and analyzing thousands of natural and synthetic diamonds collected directly from the Chinese companies, NGTC independently developed the GV5000, PL5000, DS5000, and ADD6000 instruments for rapidly screening and identifying the diamonds based on the gemological characteristics obtained.

Besides HPHT and CVD synthetic diamonds, a thickly layered hybrid diamond consisting of both natural and CVD material was identified at the NGTC Beijing laboratory (figure 1). The identification features and properties of regrown CVD synthetic diamonds using natural type Ia diamond crystals as seeds will be reported.

The current status and features of colored stones examined at NGTC laboratories, including several cases studies, will be discussed.

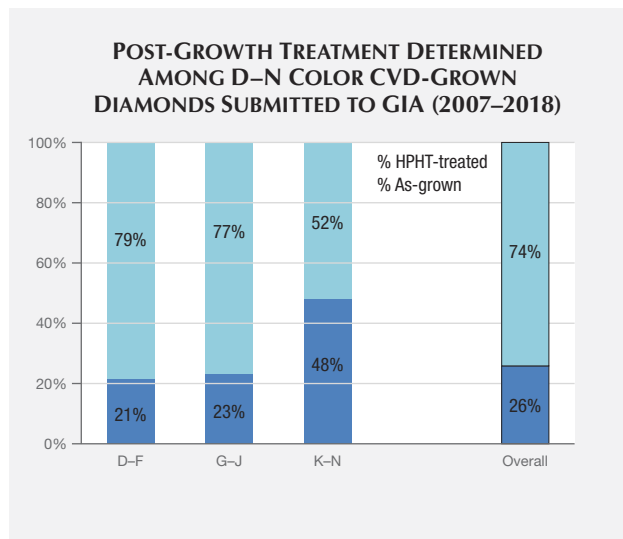
Summary of CVD Lab-Grown Diamonds Seen at the GIA Laboratory

Sally Eaton-Magaña
GIA, Carlsbad, California

While chemical vapor deposition (CVD) diamond growth technology has progressed significantly in recent years, with improvements in crystal size and quality, the use of these goods in the jewelry trade is still limited. Not all CVD-grown gem diamonds are submitted to GIA for grading reports, and they only account for about 0.01% of GIA's annual diamond intake (both D–Z equivalents and fancy color; Eaton-Magaña and Shigley, 2016). The CVD process involves diamond growth at moderate temperatures (700–1300°C) but very low pressures of less than 1 atmosphere in a vacuum chamber (e.g., Angus and Hayman, 1988; Nad et al., 2015). This presentation summarizes the quality factors and other characteristics of the CVD-grown material submitted to GIA (e.g., figure 1) and discusses new research and products.

Today the CVD process is used to produce high-color (as well as fancy-color) and high-clarity type II diamonds up to several carats in size. The majority of the CVD material seen at GIA consists of near-colorless (G–N equivalent) with colorless (D–F equivalent) and various “pink” hues. Additionally, CVD material is constantly setting new size milestones, with the announcement of an approximately 6 ct round brilliant earlier this year (Davis, 2018). However, the attainable sizes among CVD products are dwarfed by those from the HPHT process, with 15.32 ct as the current record for a faceted gem (Ardon and Eaton-Magaña, 2018).

Figure 1. Spectra and fluorescence images of all D–N equivalent CVD-grown diamonds seen at GIA from 2007 to 2018 were analyzed. The vast majority (74%) show features consistent with post-growth HPHT treatment. The percentage of as-grown CVD products increases as the equivalent color progresses from the colorless range (D–F) to near-colorless (G–J) to faint brown (K–N).

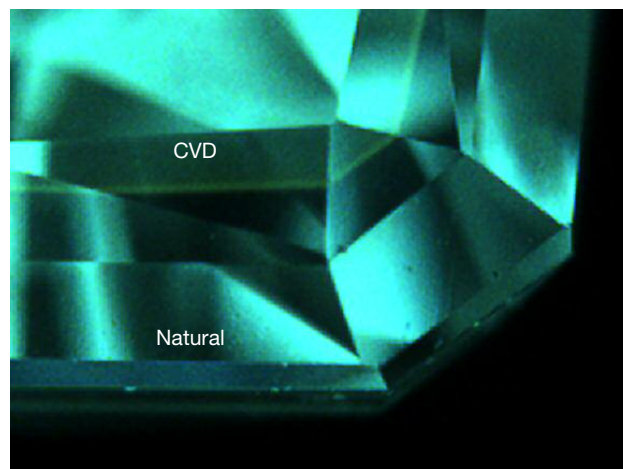


One particular challenge for gemologists (albeit very rarely encountered) comes from the lab-grown/natural hybrids (figure 2) that have been submitted to and documented by gemological laboratories (e.g., Moe et al., 2017; Tang et al., 2018). In these specimens, the grower places a *natural* diamond into the CVD reactor as the seed plate, with both components retained in the faceted gem. If the manufacturer is using a colorless natural type Ia diamond as a seed plate for near-colorless CVD growth, the hybrid cannot undergo any post-growth HPHT treatment, as this would radically alter the natural seed by turning the natural diamond yellow. If the manufacturer is creating a CVD overgrowth layer on a faceted natural diamond, the intent is to either add weight to a diamond that may be near a weight boundary or to achieve a color change, typically to blue. These hybrid products also make it more difficult to infer a diamond's history based solely on its diamond type.

The CVD process has also created some unique gems that have not been duplicated among natural, treated, or HPHT-grown diamonds. These include CVD-grown diamonds with a high concentration of silicon impurities, which create a pink to blue color shift. In those samples, a temporary effect was activated by UV exposure, which precipitated a charge transfer between negative and neutral silicon-vacancy centers (D'Haenens-Johansson et al., 2015).

Also recently seen are type IIb CVD goods. Some that were submitted by clients had a low boron concentration (3 ppb, with G-equivalent color and 1.05 carat weight). Meanwhile, some research samples produced by a manufacturer in China and fashioned as flat plates had dark bluish coloration and very high boron

Figure 2. This 0.33 ct CVD-grown/natural diamond composite with a color equivalent to Fancy blue was previously described (Moe et al., 2017). DiamondView illumination clearly shows the interface between the lab-grown and natural components.



concentration (2500 ppb and higher). Also among that suite of flat-plate CVD samples was one with a black color caused by extremely high amounts of nitrogen-vacancy centers.

REFERENCES

- Angus J.C., Hayman C.C. (1988) Low-pressure, metastable growth of diamond and diamondlike phases. *Science*, Vol. 241, No. 4868, pp. 913–921.
- Ardon T., Eaton-Magaña S.C. (2018) Lab Notes: 15 carat HPHT synthetic diamond. *G&G*, Vol. 54, No. 2, pp. 217–218.
- Davis A. (2018) Washington, D.C., company grows 6-carat diamond. *National Jeweler*, Jan. 31, <https://www.nationaljeweler.com/diamonds-gems/supply/6267-washington-d-c-company-grows-6-carat-diamond>
- D’Haenens-Johansson U.F.S., Ardon T., Wang W. (2015) CVD synthetic gem diamonds with high silicon-vacancy concentrations. *Conference on New Diamond and Nano Carbons*, May 2015, Shizuoka, Japan.
- Eaton-Magaña S.C., Shigley J.E. (2016) Observations on CVD-grown synthetic diamonds: A review. *G&G*, Vol. 52, No. 3, pp. 222–245, <http://dx.doi.org/10.5741/GEMS.52.3.222>
- Moe K.S., Johnson P., D’Haenens-Johansson U.F.S., Wang W. (2017) Lab Notes: A CVD synthetic diamond overgrowth on a natural diamond. *G&G* Vol. 53, No. 2, pp. 237–239.
- Nad S., Gu Y., Asmussen J. (2015) Growth strategies for large and high quality single crystal diamond substrates. *Diamond and Related Materials*, Vol. 60, pp. 26–34, <http://dx.doi.org/10.1016/j.diamond.2015.09.018>
- Tang S., Su J., Lu T., Ma Y., Ke J., Song Z., Zhang J., Liu H. (2018) A thick overgrowth of CVD synthetic diamond on a natural diamond. *Journal of Gemology*, Vol. 36, No. 2, pp. 237–239.

Although new CVD products are continually being manufactured and introduced to the trade, the laboratory-grown diamonds examined to date by GIA can be readily identified.

Diamond Geology

Modern Advances in the Understanding of Diamond Formation



D. Graham Pearson

University of Alberta, Edmonton, Canada

For the past 50 years, the majority of diamond research has focused on diamonds derived from the lithospheric mantle root underpinning ancient continents. While lithospheric diamonds are currently thought to form the mainstay of the world’s economic production, the continental mantle lithosphere reservoir comprises only ~2.5% of the total volume of Earth. Earth’s upper mantle and transition zone, extending from beneath the lithosphere to a depth of 670 km, occupy a volume approximately 10 times larger.

Diamonds from these deeper parts of the earth—“superdeep diamonds”—are more abundant than previously thought. They appear to dominate the high-value large diamond population that comes to market. Recent measurements of the carbon and nitrogen isotope composition of superdeep diamonds from Brazil and southern Africa, using *in situ* ion probe techniques, show that they document the deep recycling of volatile elements (C, N, O) from the surface of the earth to great depths, at least as deep as the uppermost lower mantle. The recycled crust signatures in these superdeep diamonds suggest their formation in regions of subducting oceanic plates, either in the convecting upper mantle or the transition zone plus lower mantle. It is likely that the deep subduction processes involved in forming these diamonds also transport surficial hydrogen into the deep mantle. This notion is supported by the observation of a high-pressure olivine polymorph—ringwoodite—with close to saturation levels of water. Hence, superdeep diamonds document a newly recognized, voluminous “diamond factory” in the deep earth, likely producing diamonds right up to the present day. Such diamonds

also provide uniquely powerful views of how crustal material is recycled into the deep earth to replenish the mantle’s inventory of volatile elements.

The increasing recognition of superdeep diamonds in terms of their contribution to the diamond economy opens new horizons in diamond exploration. Models are heavily influenced by the search for diamonds associated with highly depleted peridotite (dunites and harzburgites). Such harzburgitic diamonds were formed in the Archean eon (>2.5 Ga) within lithospheric mantle of similar age. It is currently unclear what the association is between these ancient lithospheric diamonds and large, high-value diamonds, but it is likely a weak one. In contrast, the strong association between superdeep diamonds and these larger stones opens up a new paradigm because the available age constraints for superdeep diamonds indicate that they are much younger than the ancient lithospheric diamonds. Their younger age means that superdeep diamonds may be formed in non-Archean mantle, or mantle that has been strongly overprinted by post-Archean events that would otherwise be deemed unfavorable for the preservation of ancient lithospheric diamonds.

An additional factor in the search for new diamond deposits is the increasing recognition that major diamond deposits can form in lithospheric mantle that is younger than—or experienced major thermal disruption since—the canonical 2.5 billion years usually thought to be most favorable for diamond production.

This talk will explore these new dimensions in terms of the potential for discovering new diamond sources in “unconventional” settings.

Diamond Precipitation from High-Density CHO Fluids

Thomas Stachel¹, Robert W. Luth¹, and Oded Navon²

¹University of Alberta, Edmonton, Canada

²Hebrew University, Jerusalem

Through research on inclusions in diamonds over the past 50 years, a detailed picture has emerged of the mineralogical and chemical composition of diamond substrates in Earth's mantle and of the pressure-temperature conditions during diamond formation. The exact diamond-forming processes, however, are still a subject of debate.

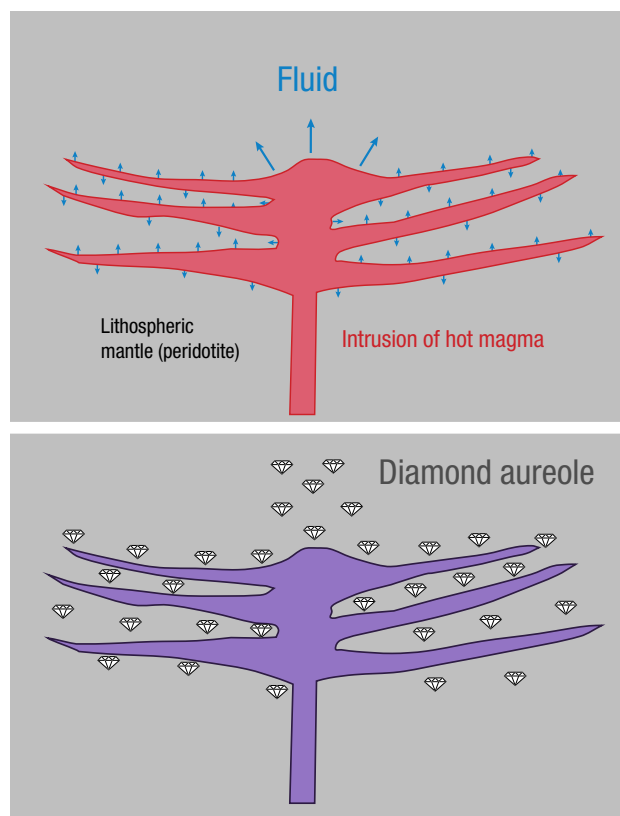
One approach to constrain diamond-forming processes is through model calculations that aim to obtain the speciation and the carbon content of carbon-hydrogen-oxygen (CHO) fluids at particular O/(O+H) ratios and pressure-temperature conditions (using GFluid of Zhang and Duan, 2010, or other thermodynamic models of fluids). The predictions of such model calculations can then be tested against carbon and nitrogen stable isotopes and nitrogen content fractionation models, based on *in situ* analyses across homogeneously grown diamond growth layers. Based on this approach, Luth and Stachel (2014) proposed that diamond precipitation occurs predominantly from cooling or ascending CHO fluids, composed of water with minor amounts of CO₂ and CH₄ (which in response to decreasing temperature may react to form diamond: CO₂ + CH₄ → 2C + 2H₂O).

The second approach focuses on constraining the diamond-forming medium by studying submicrometer fluid inclusions in fibrous-clouded and, more recently, gem diamonds. Such studies established the presence of four compositional end members of inclusions: hydrous-saline, hydrous-silicic, high-Mg carbonatitic, and low-Mg carbonatitic (e.g., Navon et al., 1988; Weiss et al., 2009). Although these fluid inclusions only depict the state of the diamond-forming medium after formation, they nevertheless provide unique insights into the major and trace-element composition of such fluids that otherwise could not be obtained.

The apparent dichotomy between the two approaches—models for pure CHO fluids and actual observation of impure fluids (so-called high-density fluids) in clouded and fibrous diamonds—relates to the observation that in high-pressure and high-temperature experiments close to the melting temperature of mantle rocks, hydrous fluids contain 10–50% dissolved solid components (e.g., Kessel et al., 2015). Although at this stage the impurity content in natural CHO fluids cannot be included in numerical models, the findings for clouded and fibrous diamonds are not in conflict with the isochemical diamond precipitation model. Specifically, the fact that observed high-density inclusions are often carbonate bearing is not in conflict with the relatively reducing redox conditions associated with the O/(O+H) ratios of modeled diamond-forming CHO fluids. The model for the minimum redox stability of carbonate-bearing melts of Stagno and Frost (2010) permits fluid carbonate contents of up to about 30% at such redox conditions.

Although additional data need to be obtained to build a thermodynamic model for CHO fluids with dissolved silicates and to better characterize the major and trace-element composition of high-density CHO fluids in equilibrium with typical diamond substrates (the rock types peridotite and eclogite), we already see sufficient evidence to suggest that the two approaches described above are converging to a unified model of isochemical diamond precipitation from cooling or ascending high-density CHO fluids.

Figure 1. This illustration depicts the isochemical precipitation of diamond in Earth's lithospheric mantle. Top: Intrusion of magma (ΔT to peridotitic wall rock is about +200°C) leads to release of hot CHO fluids from the crystallizing melt. As it infiltrates the peridotitic wall rock, the cooling fluid isochemically precipitates diamond. Bottom: After crystallization of the melt is completed, the intrusion is surrounded by an aureole of diamond, with temperature, volume, fluid content, and redox state of the melt all influencing the amount of diamond precipitated.



REFERENCES

- Kessel R., Fumagalli P., Pettko T. (2015) The behaviour of incompatible elements during hydrous melting of metasomatized peridotite at 4–6 GPa and 1000°C–1200°C. *Lithos*, Vol. 236–237, pp. 141–155, <https://doi.org/10.1016/j.lithos.2015.08.016>
- Luth R.W., Stachel T. (2014) The buffering capacity of lithospheric mantle: implications for diamond formation. *Contributions to Mineralogy and Petrology*, Vol. 168, No. 5, pp. 1–12, <https://doi.org/10.1007/s00410-014-1083-6>
- Navon O., Hutcheon I.D., Rossman G.R., Wasserburg G.J. (1988) Mantle-derived fluids in diamond micro-inclusions. *Nature*, Vol. 335, No. 6193, pp. 784–789, <https://doi.org/10.1038/335784a0>
- Stagno V., Frost D.J. (2010) Carbon speciation in the asthenosphere: Experimental measurements of the redox conditions at which carbonate-bearing melts coexist with graphite or diamond in peridotite assemblages. *Earth and Planetary Science Letters*, Vol. 300, No. 1–2, pp. 72–84, <https://doi.org/10.1016/j.epsl.2010.09.038>
- Weiss Y., Kessel R., Griffin W.L., Kiflawi I., Klein-BenDavid, O., Bell D.R., Harris J.W., Navon O. (2009) A new model for the evolution of diamond-forming fluids: Evidence from microinclusion-bearing diamonds from Kankan, Guinea. *Lithos*, Vol. 112 (Supplement 2), pp. 660–674, <https://doi.org/10.1016/j.lithos.2009.05.038>
- Zhang C., Duan Z.H. (2010) GFluid: An Excel spreadsheet for investigating C-O-H fluid composition under high temperatures and pressures. *Computers & Geosciences*, Vol. 36, No. 4, pp. 569–572, <https://doi.org/10.1016/j.cageo.2009.05.008>

How to Obtain and Interpret Diamond Ages

Steven B. Shirey¹ and D. Graham Pearson²

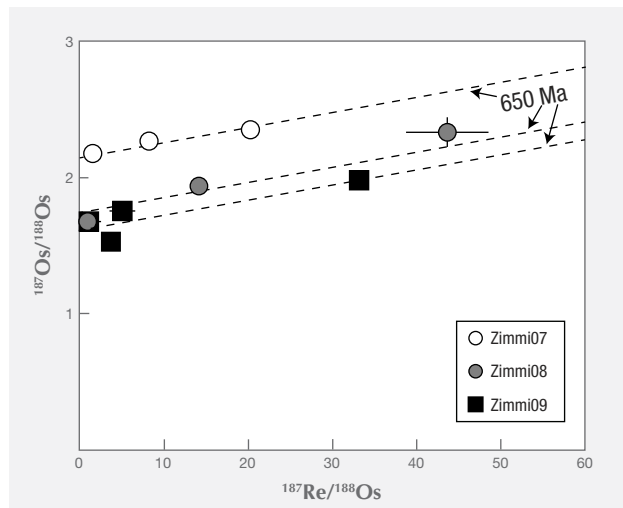
¹Carnegie Institution for Science, Washington, DC

²University of Alberta, Edmonton, Canada

Diamond ages are obtained from radiogenic isotopic analysis (Rb-Sr, Sm-Nd, Re-Os, and Ar-Ar) of mineral inclusions (garnet, pyroxene, and sulfide). As diamonds are xenocrysts that cannot be dated directly, the ages obtained on mineral inclusions provide a unique set of interpretive challenges to assure accuracy and account for preexisting history. A primary source of geological/mineralogical uncertainty on diamond ages is any process affecting protogenetic mineral inclusions before encapsulation in the diamond, especially if it occurred long before diamond formation. In practical application, the isotopic systems discussed above also carry with them inherent systemic uncer-

tainties. Isotopic equilibrium is the essential condition required for the generation of a statistically robust isochron. Thus, isochron ages from multiple diamonds will record a valid and accurate age when the diamond-forming fluid promotes a large degree of isotopic equilibrium across grain scales, even for preexisting (“protogenetic”) minerals. This clearly can and does occur. Furthermore, it can be analytically tested for, and has multiple analogues in the field of dating metamorphic rocks. In cases where an age might be suspect, an age will be valid if its regression uncertainties can encompass a known and plausible geological event (especially one for which an association exists between that

Figure 1. Left: Re-Os isotopic compositions for 10 sulfides from three Zimmi diamonds all fall along 650 Ma age arrays. Each diamond had multiple sulfides that lay on arrays of identical age, giving unequivocal evidence for the age and showing that these diamonds formed in the same episode of diamond formation. Right: Plane polarized light image of a typical sulfide inclusion in a polished Zimmi diamond plate. Note that this diamond only contains one inclusion, whereas analyses of three to four inclusions per diamond are shown in the plot on the left. From Smit et al. (2016), used with permission.



event and the source of diamond-forming fluids) and petroge-
netic links can be established between inclusions on the isochron.

Diamonds can be dated in six basic ways:

1. model ages
2. radiogenic daughter Os ages (common-Os-free)
3. single-diamond mineral isochrons
4. core to rim ages
5. multiple single-diamond isochron/array ages
6. composite isochron/array ages

Model ages (1) are produced by the intersection between the evolution line for the inclusion and a reference reservoir such as the mantle. The most accurate single-diamond age is determined on a diamond with multiple inclusions (3). In this case an internal

isochron can be obtained that not only establishes equilibrium among the multiple grains but also unequivocally dates the time of diamond growth. With extreme luck in obtaining the right diamond, concentric diamond growth zones visible in UV fluorescence or cathodoluminescence can sometimes be shown to constrain inclusions to occur in the core of the diamond and in the exterior at the rim. These single grains can be extracted to give a minimum growth time (4) for the diamond. In optimal situations, multiple inclusions are present within single growth zones, in single diamonds, allowing internal isochrons to be constructed for individual growth zones in single diamonds. If enough diamonds with inclusions can be obtained for study, valid ages for diamond populations can be obtained on multiple single-diamond ages that agree (5) or on composited, mineralogically similar inclusions to give an average age (6).

REFERENCE

Smit K.V., Shirey S.B., Wang W. (2016) Type Ib diamond formation and preservation in the West African lithospheric mantle: Re–Os age constraints from

sulphide inclusions in Zimmi diamonds. *Precambrian Research*, Vol. 286, pp. 152–166, <http://dx.doi.org/10.1016/j.precamres.2016.09.022>

The Lesedi La Rona and the Constellation— The Puzzle of the Large Rough Diamonds from Karowe

Ulrika F.S. D'Haenens-Johansson
GIA, New York

In November 2015, Lucara Diamond's operation at the Karowe mine in Botswana gained notoriety due to the extraction of a series of large colorless diamonds, including the 1,109 ct Lesedi La Rona and the 812 ct Constellation. The Lesedi La Rona marks the largest gem diamond recovered since the Cullinan (3,106 ct) in 1905. The Constellation, considered to be the seventh-largest recorded diamond, attained the highest price ever paid for a rough, selling for \$63.1 million (\$77,649 per carat). Additionally, three other significant colorless diamonds were recovered during the same period, weighing 374, 296, and 183 ct. Due to the similarity in their external characteristics—which include cleavage faces—as well as their extraction locations and dates, it was suspected that these stones might have originated from a larger rough that had broken. Lucara demonstrated that the 374 ct diamond and the Lesedi La Rona fit together, yet a large cleavage plane is still unaccounted for. GIA was able to study several rough and/or faceted pieces of these five diamonds using a range of spectroscopic and imaging techniques to gain insight into the presence and distribution of point defects in these diamonds.

Diamonds are commonly classified according to their nitrogen content measured by Fourier-transform infrared (FTIR) spectroscopy: Type I diamonds contain nitrogen in either isolated (Ib) or aggregated (IaAB) forms, while type II diamonds do not contain detectable nitrogen concentrations (IIa) but may contain boron (IIb). Analysis of faceted stones cut from the Lesedi La Rona indicates that the rough is a mixed-type diamond, containing both type

IIa and pure type IaB regions. These types of diamonds, though exceedingly unusual, have been observed at GIA and reported by De-launay and Fritsch (2017). The Constellation and the 374, 296, and 183 ct diamonds were determined to be type IaB, containing 20 ± 4 ppm B-aggregates (N_4V), in agreement with the concentration for the type IaB pieces of the Lesedi La Rona. Pure type IaB diamonds such as these are actually quite rare, accounting for only 1.2% of a random suite of 5,060 large (>10 ct) D-to-Z diamonds submitted to GIA, whereas 24.6% were type II. Photoluminescence spectra further confirmed analogous defect content for the five large Karowe diamonds, with emissions from H4 ($N_4V_2^0$, 496 nm), H3 (NVN^0 , 503 nm), 505 nm, NV^- (637 nm), and GR1 (V^0 , 741 nm) defects showing similar relative intensities and peak widths. Even for diamonds of the same type, parallel defect content and characteristics across such a variety of defects is unlikely for unrelated stones.

The external morphologies of the diamonds showed primary octahedral, resorbed, and fractured faces, with the Constellation and the 296 ct diamond featuring fractures containing metallic inclusions and secondary iron oxide staining. Deep UV fluorescence (<230 nm) imaging elucidated the internal growth structures of the samples. For the Constellation and the 374, 296, and 183 ct diamonds, at least two growth zones with differing blue fluorescence intensities were observed within single pieces.

Combined with the spectroscopic data, these results provide

compelling evidence that the Lesedi La Rona, the Constellation, and the 374, 296, and 183 ct diamonds from Karowe had com-

parable growth histories and likely originated from the same rough, with a combined weight of at least 2,774 ct.

REFERENCE

Delaunay A., Fritsch E. (2017) A zoned type IaB/IIa diamond of probable “superdeep” origin. *Journal of Gemmology*, Vol. 35, No. 5, pp. 397–399.

Gem Characterization

The Formation of Natural Type IIa and IIb Diamonds

Evan M. Smith and Wuyi Wang

GIA, New York

Many of the world’s largest and most valuable gem diamonds exhibit an unusual set of physical characteristics. For example, in addition to their conspicuously low nitrogen concentrations, diamonds such as the 3,106 ct Cullinan (type IIa) and the Hope (type IIb, boron bearing) tend to have very few or no inclusions, and in their rough state they are found as irregular shapes rather than as sharp octahedral crystals. It has long been suspected that type IIa and IIb diamonds form in a different way than most other diamonds.

Over the past two years, systematic investigation of both type IIa and IIb diamonds at GIA has revealed that they sometimes contain rare inclusions from unique geological origins. Examination of more than 130 inclusion-bearing samples has established recurring sets of inclusions that clearly show many of these diamonds originate in the sublithospheric mantle, much deeper in the earth than more common diamonds from the cratonic lithosphere. We now recognize that type IIa diamonds, or more specifically, diamonds with characteristics akin to the historic Cullinan diamond (dubbed CLIPPIR diamonds), are distinguished by the occurrence of iron-rich metallic inclusions. Less frequently, CLIPPIR diamonds also contain inclusions of majoritic garnet and former CaSiO_3 perovskite that constrain the depth of formation to within 360–750 km. The inclusions suggest that CLIPPIR diamonds belong to a unique paragenesis with an intimate link to metallic iron in the deep mantle (Smith et al., 2016, 2017). Similarly, findings from type IIb diamonds also place them in a “superdeep” sublithospheric mantle setting, with inclusions of former CaSiO_3 perovskite and other high-pressure minerals, although the iron-rich metallic inclusions are generally absent (Smith et al., 2018). Altogether, these findings show that high-quality type II gem diamonds are predominantly sourced from the sublithospheric mantle, a surprising result that has

refuted the notion that all superdeep diamonds are small and non-gem quality. Valuable information about the composition and behavior of the deep mantle is cryptically recorded in these diamonds. CLIPPIR diamonds (figure 1) confirm that the deep mantle contains metallic iron, while type IIb diamonds suggest that boron and perhaps water can be carried from the earth’s surface down into the lower mantle by plate tectonic processes. In addition to being gemstones of great beauty, diamonds carry tremendous scientific value in their unique ability to convey information about the interior of our planet.

Figure 1. Measuring about 7 cm across, this 404.2 ct rough from Angola’s Lulo mine is a good example of the irregular shape and surface texture associated with CLIPPIR diamonds. The unusual characteristics of diamonds like this one are the result of formation in a unique geological setting. Once cut, this rough yielded a 163.4 ct flawless D-color diamond. Photo by Jian Xin (Jae) Liao.



REFERENCES

Smith E.M., Shirey S.B., Nestola F., Bullock E.S., Wang J., Richardson S.H., Wang W. (2016) Large gem diamonds from metallic liquid in Earth’s deep mantle. *Science*, Vol. 354, No. 6318, pp. 1403–1405, <http://dx.doi.org/10.1126/science.aal1303>

Smith E.M., Shirey S.B., Wang W. (2017) The very deep origin of the world’s biggest diamonds. *G&G*, Vol. 53, No. 4, pp. 388–403, <http://dx.doi.org/>

10.5741/GEMS.53.4.388

Smith E.M., Shirey S.B., Richardson S.H., Nestola F., Bullock E.S., Wang J., Wang W. (2018) Blue boron-bearing diamonds from Earth’s lower mantle, *Nature*, Vol. 560, No. 7716, pp. 84–87, <http://dx.doi.org/10.1038/s41586-018-0334-5>



Colored Diamonds: The Rarity and Beauty of Imperfection

Christopher M. Breeding
GIA, Carlsbad, California

Diamond is often romanticized as a symbol of purity and perfection, with values that exceed all other gemstones. However, even the most flawless and colorless natural diamonds have atomic-level imperfections. Somewhat ironically, the rarest and most valuable gem diamonds are those that contain abundant impurities or certain atomic defects that produce beautiful fancy colors such as red, blue, or green—stones that can sell for millions of dollars per carat.

Atomic defects can consist of impurities such as nitrogen or boron that substitute for carbon atoms in the diamond atomic structure (resulting in classifications such as type Ia, type Ib, type IIa, and type IIb) or missing or misaligned carbon atoms. Some defects are created during diamond growth, while others are generated over millions to billions of years as the diamond sits deep in the earth at high temperatures and pressures. Defects may be created when the diamond is rapidly transported to the earth's surface or by interaction with radioactive fluids very near the earth's surface. Each defect selectively absorbs different wavelengths of light to produce eye-visible colors. Absorptions from these color-producing defects (or color centers) are detected and identified using the gemological spectroscope or more sensitive absorption spectrometers such as Fourier-transform infrared (FTIR) or ultraviolet/visible/near-infrared (UV-Vis-NIR; figure 1). Some defects not only absorb light but also produce their own luminescence, called fluorescence. For example, the same defect that produces “cape” yellow diamonds also generates blue fluorescence when exposed to ultraviolet light. In some cases, the fluorescence generated by defects can be strong enough to affect the color of gem diamonds.

Figure 1. Visible-NIR spectra reveal the absorptions and corresponding atomic defects responsible for the color in gem diamonds.

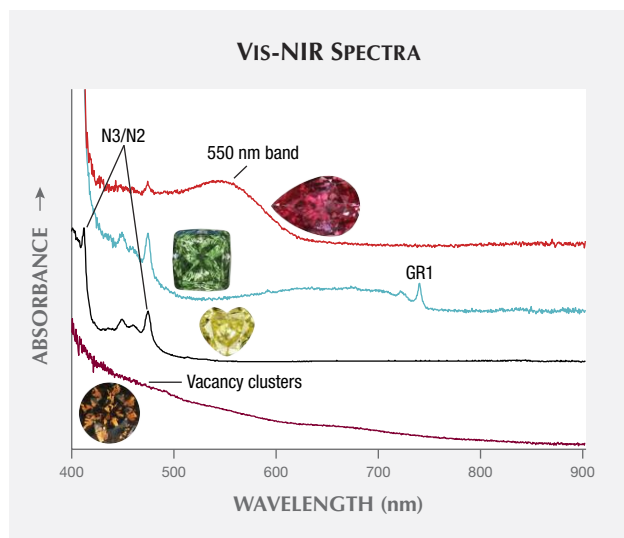


TABLE 1. Most common causes of color in gem diamond.

Color	Cause of color (defect structure)	When imparted
Yellow	N3/N2 “cape” (3NV)	Residence at high T and P
	Isolated nitrogen “C centers” (N)	Growth
	H3 absorption (2NV ⁰)	Residence at high T and P
	Hydrogen (unknown)	Growth
	480 nm band (unknown)	Growth? (unknown origin)
Brown	Vacancy clusters (multiple V)	Transport/residence at high T and P
	Isolated nitrogen “C centers” (N)	Growth
	H3 absorption (2NV ⁰) + 550 nm band (unknown)	Residence at high T and P
	Hydrogen (unknown)	Growth
Orange	H3 absorption (2NV ⁰) + 550 nm band (unknown)	Transport/residence at high T and P
	480 nm band (unknown)	Growth? (unknown origin)
	Isolated nitrogen “C centers” (N)	Growth
Red/Pink	Plastic deformation—550 nm band (unknown)	Transport/residence at high T and P
	Nitrogen-vacancy (NV ⁰ , NV ⁻)	Residence at high T and P
Violet/Purple	Hydrogen (unknown)	Growth
	Plastic deformation—550 nm band (unknown)	Transport/residence at high T and P
Green	Radiation damage—GR1 (V ⁰)	Radioactive fluids—low T and P
	H3 fluorescence (2NV ⁰)	Residence at high T and P
	Hydrogen (unknown)	Growth
	Nickel (Unknown)	Growth
Blue	Boron (B)	Growth
	Radiation damage—GR1 (V ⁰)	Radioactive fluids—low T and P
	Hydrogen (unknown)	Growth

With the exception of most natural white and black diamonds, where the color is a product of inclusions, colored diamonds owe their hues to either a single type of defect or a combination of several color centers. More than one type of defect can produce a particular color, however. Table 1 provides a list of the most common causes of color in diamond.

Subtle differences in atomic defects can drastically affect a diamond's color. For example, isolated atoms of nitrogen impurities usually produce strong yellow color (“canary” yellow diamonds). If those individual nitrogen atoms occur together in pairs, no color is generated and the diamond is colorless. If instead the individual nitrogen atoms occur adjacent to missing carbon atoms (vacancies), the color tends to be pink to red. Rearrangement of diamond defects is the foundation of using treatments to change the color of diamond. Identification of treatments and separation of natural and synthetic diamond requires a thorough understanding of the atomic-level imperfections that give rise to diamond color and value.

Evaluating the Color and Nature of Diamonds Via EPR Spectroscopy

Haim Cohen¹ and Sharon Ruthstein²

¹Ariel University and Ben-Gurion University of the Negev, Israel

²Bar-Ilan University, Israel

Diamond characterization is carried out via a wide variety of gemological and chemical analyses. An important analytical tool for this purpose is spectroscopic characterization utilizing both absorption and emission measurements. The main techniques are UV-visible and infrared spectroscopy, though Raman as well as cathodoluminescence spectroscopy are also used.

We have used electron paramagnetic resonance (EPR) spectroscopy to compare the properties of treated colored diamonds to the pretreated stones. The colors studied were blue, orange, yellow, green, and pink. The EPR technique determines radicals (atoms with unpaired electrons) and is very sensitive, capable of measuring concentrations as low as $\sim 1 \times 10^{-17}$ radicals/cm³. The results, shown in table 1, indicate that all the carbon radicals determined are affected by adjacent nitrogen atoms, with the spectra showing a hyperfine structure attributed to the presence of nitrogen. The highest concentration of radicals and hyperfine structures is observed in pink and orange treated diamonds. The results concerning nitrogen concentration were correlated with

TABLE 1. Distribution of radical concentration in treated colored diamonds.

Blue	40% N	60% C	
Orange	2% N	98% C	
Yellow	8% N	92% C	
Green	2% N	98% C	
Pink	1.8% N	98.2% C	

the infrared spectra, which determine the absorption peaks of the diamonds as well as those of the nitrogen contamination in their crystal structure.

Quantitative Absorption Spectrum Reconstruction for Polished Diamond

Roman Serov (presented by Sergey Sivovolenko)

OctoNus Software, Moscow

Natural diamonds generally exhibit a very wide range of spectra. In polished stones, absorption along with proportions and size define perceived diamond color and thus beauty.

In rough diamonds, the quantitative absorption spectrum (the “reference spectrum” in the context of this article) can be measured using an optical spectrometer through a set of parallel windows polished on a stone, so the diamond can be considered a plane-parallel plate with known thickness.

Polished diamonds lack the parallel facets that might allow plane-parallel plate measurement. That is why polished diamond colorimetry uses one of two approaches that have certain limitations for objective color estimation:

- *Qualitative spectrum assessment with an integrating sphere.* Suppose three diamonds are polished from a yellow rough with even coloration: a round (with short ray paths), a cushion (with high color uniformity and long ray paths), and a “bow tie” marquise (with both long and short ray path areas). The spectra captured from these three stones by an integrating sphere will be completely different because the ray paths are very different. However, the quantitative absorption spectrum will be the same for all three stones, since they are cut

from the same evenly colored rough. Therefore, spectrum assessment with an integrating sphere has very limited accuracy and is practical for qualitative estimations only.

- *Analysis of multiple images of a diamond made by color RGB camera.* This method has low spectral resolution defined by digital camera color rendering. The camera has a smaller color gamut than the human eye, so most fancy-color diamonds are outside the color-capturing range of a digital camera.

However, quantitative absorption data is very valuable for:

- Color prediction and optimization for a new diamond after a recut process
- Objective color assessment and description of a polished diamond

This paper presents a new technology based on spectral light-emitting diodes (LEDs) and high-quality ray tracing, which together allow the reconstruction of a quantitative absorption spectrum for a polished diamond. The approach can be used for any transparent polished diamond. The recent technology prototype has a resolution of 20–60 nm, which is practical for color assessment.

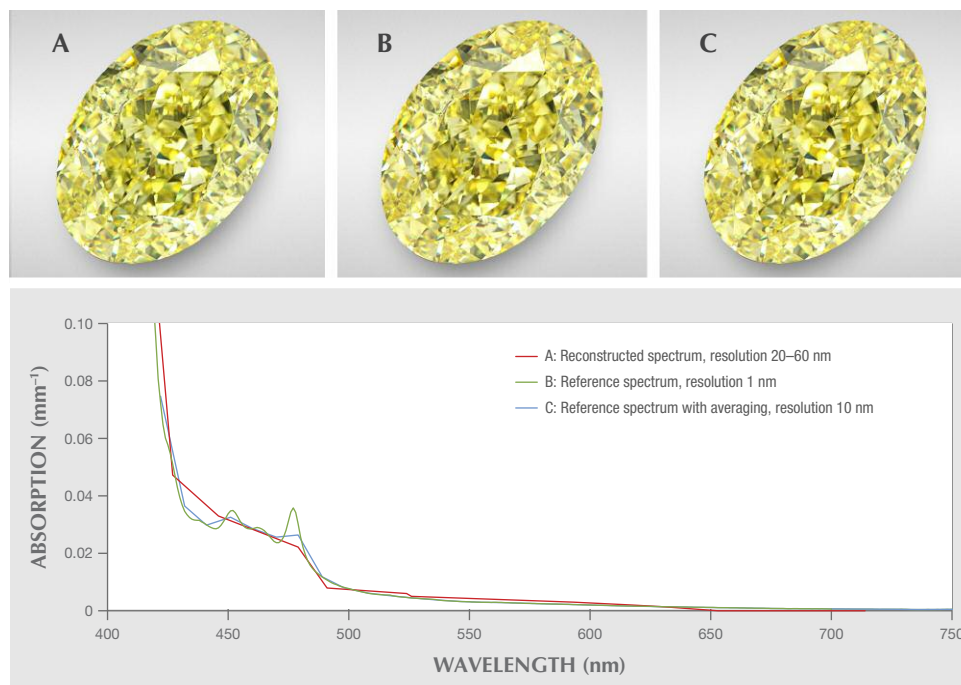


Figure 1. Top: Photorealistic diamond images generated from the reconstructed absorption spectrum (A), the reference spectrum (B), and the averaged reference spectrum (C) of the same stone. Bottom: Quantitative and reconstructed absorption spectra.

Figure 1 (top) presents three photorealistic diamond images: A is based on the reconstructed absorption spectrum collected from a polished diamond, B uses the reference spectrum collected in the rough stage through a pair of parallel windows, and C uses the averaged reference spectrum. Figure 1 (bottom) shows both measured

quantitative absorption and reconstructed absorption spectra.

This technology has the potential to ensure very close to objective color estimation for near-colorless and fancy-color polished diamonds. The reconstructed spectrum resolution can be enhanced to 10–15 nm in future devices.

Gem Localities

Scientific Study of Colored Gem Deposits and Modern Fingerprinting Methods

Lee Groat

University of British Columbia, Vancouver, Canada

Most colored gemstones form near the earth's surface in a wide range of different environments; for example, they can crystallize from igneous magmas or hydrothermal solutions, or via the recrystallization of preexisting minerals during metamorphism. The specific environment determines the types of gem minerals that form, as well as their physical and chemical properties. Field studies of colored gem deposits provide the basis for the scientific understanding of natural gemstone formation and, in turn, the basis for gem identification.

Gem deposits are of scientific interest because they represent unusual geologic and geochemical conditions; for example, emeralds are rare because they require beryllium and chromium (and/or vanadium), which generally travel in very different geochemical circles. Scientists study gem deposits by collecting rock and mineral samples in the field, mapping geological formations and structures, documenting the environment in which the gems

occur, and examining the collected samples back in the laboratory. Such examination yields information on the chemical, temperature, and pressure conditions of gem formation, the associated minerals (often found as distinctive inclusions in the gems themselves), and the age of the deposit. Determining the origin of a gem deposit usually requires a small amount of very specific data. The results are published in publicly available peer-reviewed publications. Such field studies provide clues that can be used to explore for similar types of gem deposits. Challenges include the remoteness of locations that have not been previously studied by geologists, the small size of deposits that precludes study by large mining companies, and the rarity of the gems themselves.

There is much left to do in gem deposit research. For example, despite its growing popularity as a gemstone, there are few studies of gem spinel deposits, especially cobalt-blue spinel (figure 1), for



which only one deposit has been studied. To date we know little about what factors control spinel genesis and color.

Recently there has been another reason to study gem deposits: gem fingerprinting, in which modern methods are used to obtain characteristic information. This information is then compared to information obtained from stones from known localities to estimate where a stone with no locality information originated.

Modern fingerprinting methods analyze the chemistry of the stones (using electron probe microanalysis, isotopic analysis, laser ablation–inductively coupled plasma–mass spectrometry) and/or their solid and fluid inclusions. We know that the chemistry of the stones must reflect the chemistry of the host rock environment; for example, the chromophore in emerald from Lened in Canada is vanadium, and not the typical chromium, because there are no chromium-bearing rocks in the area. With respect to solid inclusions, rubies from Aappaluttoq in Greenland have phlogopite mica inclusions because they recrystallized in a rock at pressures and temperatures where phlogopite is the stable potassium-bearing phase. An example of diagnostic fluid inclusions is the three-phase variety seen in Colombian emeralds (and now also observed elsewhere). New is the use of ICP-MS on fluid inclusions to define part of the fluid assemblage from which the stones were formed; this tells us about the environment of formation, but also may assist in defining a fingerprint for the stone.

Where scientific studies require only very specific data, the more data available from stones of known origin, and the more representative those stones are of the full range of compositions



Figure 1. Cobalt-blue gem spinel from Baffin Island, Nunavut, Canada. Photo by Lee Groat.

and inclusions found in a specific deposit or country of origin, the more accurate the estimation should be. Unfortunately, these data are generally not made public, so every lab doing fingerprinting is essentially working independently, and there is no way to know how accurate their data and the resulting country- or deposit-of-origin estimates are. We also note that a serious problem in origin determination is that some of the best gemstones will be lacking diagnostic inclusions altogether, which then restricts the tools and observations can be used.

Gem Pegmatites of Ukraine, Russia, Afghanistan, and Pakistan: An Update on Recent World-Class Finds

Peter Lyckberg

National Museum of Natural History, Luxembourg

Soviet-era exploration and mining of some 1,900 chamber pegmatites on the western endo-contact of the 1.7 Ga Korosten Pluton in Ukraine for piezo quartz left an underground mine with 110 km tunnels reached by six shafts. Since 1995, increasingly intensified study of old pockets and documentation by Vsevolod Chournousenko, chief geologist of Volhyn Kwarts (Quartz) Samotsvety Company, has revealed new targets. Work on these targets has produced gem-quality beryl and topaz, the latter in record-size crystals up to 230 and 325 kg. Topaz occurred in around 10% of mined pockets.

For the first time in the history of the huge deposit, the “Peter’s Dream Pocket” was found and exploited from January 2013 through January 2014. It contained bicolor topaz still *in situ* growing on cleavelandite, associated with zinnwaldite and smoky quartz. The largest topaz, at 325 kg, was named *dedushka* (grandfather). The Skorkina pocket in the mine was also called “Vsevolod’s Pocket” after

the extraordinary chief geologist who found the topaz mineralization, which yielded a record amount of gem topaz crystals. These came from a depth of 6 to 15 m under the floor, where previous Soviet quartz mining efforts had missed them. The largest of these, the cognac-colored “Sergei” (named after the mine owner), weighs 230 kg and is the largest of its kind. Gem-quality bicolor topaz in large sizes, found particularly in shaft 3 and in open pits in the south and north end of the pegmatite field, is unique to this mine. Extraordinary heliodor crystals were mined in Soviet times, and a smaller quantity mined later yielded faceted stones up to 2,500 ct. A recently mined deep cognac-colored cut topaz weighed 9,000 ct. Natural blue and bicolor topaz (figure 1) have been cut to unique stones, also of large sizes. The color spectrum of topaz and beryl from these pegmatites is amazing.

Lyckberg et al. (2009) noted that gem beryl occurs in only 2% of the approximately 1,900 chamber pegmatites that were mined.

Pegmatite 521 at 90 m depth, accessed from shaft 2, produced over two tons of gem beryl. Over one ton was exploited in 1982 and in 1992, over the course of five days, five miners excavated 900 kg in a green clay zone. Ninety percent of these specimens were of gem quality. In the same pegmatite, a second pocket produced 100 tons of quartz in the 1980s. During the spring of 2018, exploration of this pocket yielded a giant quartz crystal measuring 1.5 m in diameter. The pocket was found to also contain topaz pseudomorphs.

In neighboring Russia, gem aquamarine was produced in 2017 at Sherlova Mountain and sold to China, while in the Ural Mountains only small quantities for collectors were found. Here the last Russian underground gem pegmatite mine, the Kazionnitsa, closed in 1993. In the Malkhansk Mountains, tourmaline-rich lithium pegmatites with quality rubellite crystals were recovered during 2012–2018 at the Sosedka pegmatite. They were a deep red to purplish red color in crystals up to 35 cm in matrix, while gem-quality specimens measured up to 10–15 cm. Many of these crystals are reminiscent of the rubellite from the Jonas mine in Brazil, although the cranberry red color is not quite as intense. Several other pegmatite veins started to produce again, primarily green tourmaline.

The Hindu Kush pegmatites of Afghanistan discovered at Kala and Paprok villages in 1959 and 1969 have again yielded large quantities of gem tourmaline in a rainbow of colors. The huge Mawi and Kanakana pegmatites both produced large quantities of gem kunzite, gem indicolite, and rare morganites. Gem-quality pollucite and other rare species such as manganotantalite were found at Paprok and in the Pech Valley. Kanakana and several other pegmatites produced large morganites with aquamarine cores in crystals up to 25 cm in diameter growing on lepidolite and cleavelandite. The pegmatite field of Waygal produced perhaps the finest single 7 kg kunzite crystal of any find, a flawless 55 cm twinned deep purple crystal with blue 10 cm termination in a pocket with 10 kg other gem-quality crystals.

The Karakorum Mountains of Pakistan have continued to produce large quantities of aquamarine and champagne-colored topaz. Please note that beryl and topaz in these very young 4 to 12 Ma pegmatites have not yet been exposed to radiation from K40 in the feldspars or from U/Th-containing minerals during this short time span. Thus, deeply colored yellow heliodor, blue topaz, and deep or-



Figure 1. This naturally bicolored topaz, measuring 15 cm across, has eye-visible white fluorite inclusions. It was mined from pegmatite 253 (open pit) in 2017. Photo by Albert Russ, courtesy of Volhyn Kwarts (Quartz) Samotsvety Company.

ange topaz are not to be expected here, simply because they have not had a chance to attain those colors (Unpublished data by the author, 1997). Those colors are typical for pegmatites one or two magnitudes older.

Gem-quality rare species mined include large colorless to light lilac gem pollucite (10–40 cm), amblygonite, manganotantalite, various microlites, triplite, green hydroxylherderite, beryllonite in cogwheel crystals up to 35 cm, and värynenite in orange-red gem crystals up to 22 cm long. The area around Shengus and Bulochi, by the Indus River between Nanga Parbat and Haramosh Peak, is the main producer of the rarer species. Since 1985, known hydrothermal mica-lined fissures at Chumar Bakhloor (Unpublished data by the author, 1988; Lyckberg et al., 2013) have been a major source of matrix aquamarine specimens, large crystals for carvings, and much cabochon and bead material, as well as large pink and green gem-quality fluorite, some of which have been faceted.

REFERENCES

- Lyckberg P., Chournousenko V.A., Wilson W.E. (2009) Famous mineral localities: Volodarsk-Volhynsk, Zhitomit Oblast, Ukraine. *The Mineralogical Record*, Vol. 13, No. 6, pp. 11–22.
- Lyckberg P., Chournousenko V., Hmyz A. (2013) Chamber pegmatites of Volodarsk, Ukraine, the Karelia beryl mine, Finland and shallow depth vein peg-

matites of the Hindukush-Karakorum mountain ranges. Some observations on formation, inner structures, rare and gem crystals in these oldest and youngest pocket carrying gem pegmatites on Earth. In *Contributions to the 6th International Symposium on Granitic Pegmatites*, pp. 81–83, http://pegmatology.uno.edu/news_files/PEG2013_Abstract_Volume.pdf

A Multidisciplinary Approach Toward Examining the Sources of Emeralds

Raquel Alonso-Perez¹, Adriana Heimann-Rios², James M.D. Day³, Daniel X. Gray², Antonio Lanzirotti⁴, Darby D. Dyar⁵, and J.C. "Hanco" Zwaan⁶

¹Harvard University, Cambridge, Massachusetts

²East Carolina University, Greenville, North Carolina

³Scripps Institution of Oceanography, La Jolla, California

⁴The University of Chicago, Argonne, Illinois

⁵Mount Holyoke College, South Hadley, Massachusetts

⁶Naturalis Biodiversity Center (National Museum of Natural History), Leiden, The Netherlands

Modern analytical capabilities now allow the combination of non-destructive geochemical and structural studies of emeralds, in addition to detailed studies of their inclusions, to enhance our knowledge of their genesis. Here we present a combination of (1) X-ray absorption near-edge structure (XANES), to determine local coordination environment and oxidation state of the main emerald chromophores Fe, V, and Cr; (2) Raman spectroscopy, with special emphasis on the correlation between H₂O molecules and alkali site occupancy; and (3) inductively coupled plasma–mass spectrometry (solution-ICP-MS) to examine the role of major, minor, and trace elements during emerald formation. Our aim is to develop a systematic approach to characterizing emeralds by identifying key geochemical and structural features that enable provenance and geological origin of emerald deposits to be determined.

In this study, we analyzed 31 emeralds from the Mineralogical & Geological Museum, Harvard University. Preliminary XANES results indicate that chromium is present as Cr³⁺, although crystal orientation dependence and beryl crystal structural behaviors need to be assessed in detail. Raman spectroscopy results of the OH-stretching vibrations at higher frequencies (3500–3700 cm⁻¹), corresponding to H₂O type II and type I, respectively, display an orientation dependence. For a given orientation, there is an increase in intensity of the OH-stretching vibration, and therefore H₂O concentration, from Colombian to Zambian emeralds. A strong correlation of peak shape and position of the OH-stretching vibration with three major geochemical indices is also observed. Vanadium concentrations correlate positively with Ge, Rb, Cs, and Lu, and they can be used to distinguish three emerald groups based on their geochemistry: (1) Colombia; (2) South Africa, Nigeria, and Egypt; and (3) Brazil, Madagascar, and Zambia. Whereas a smooth transition occurs from group 2 to group 3, group 1 Colombian emeralds are highly distinctive. The distinctiveness of Colombian emerald indicates the potential for using trace-element abundances to examine geological formation (see figure 1). For example, ratios such as Ga/Rb versus Hf/Ta are also characteristic of each different emerald formation. The combination of XANES, Raman spectroscopy, and ICP-MS studies offers significant utility for not only refining the crystal structure of emeralds but also defining markers for different sources.

For a given orientation, there is an increase in intensity of the OH-stretching vibration, and therefore H₂O concentration, from Colombian to Zambian emeralds. A strong correlation of peak shape and position of the OH-stretching vibration with three major geochemical indices is also observed. Vanadium concentrations correlate positively with Ge, Rb, Cs, and Lu, and they can be used to distinguish three emerald groups based on their geochemistry: (1) Colombia; (2) South Africa, Nigeria, and Egypt; and (3) Brazil, Madagascar, and Zambia. Whereas a smooth transition occurs from group 2 to group 3, group 1 Colombian emeralds are highly distinctive. The distinctiveness of Colombian emerald indicates the potential for using trace-element abundances to examine geological formation (see figure 1). For example, ratios such as Ga/Rb versus Hf/Ta are also characteristic of each different emerald formation. The combination of XANES, Raman spectroscopy, and ICP-MS studies offers significant utility for not only refining the crystal structure of emeralds but also defining markers for different sources.

REFERENCE

Rudnick R.L., Gao S. (2004) Composition of the continental crust. In H.D. Holland and K.K. Turekian, Eds., *Treatise on Geochemistry. Vol. 3, The Crust*, Elsevier-Pergamon, Oxford, UK, pp. 1–64.

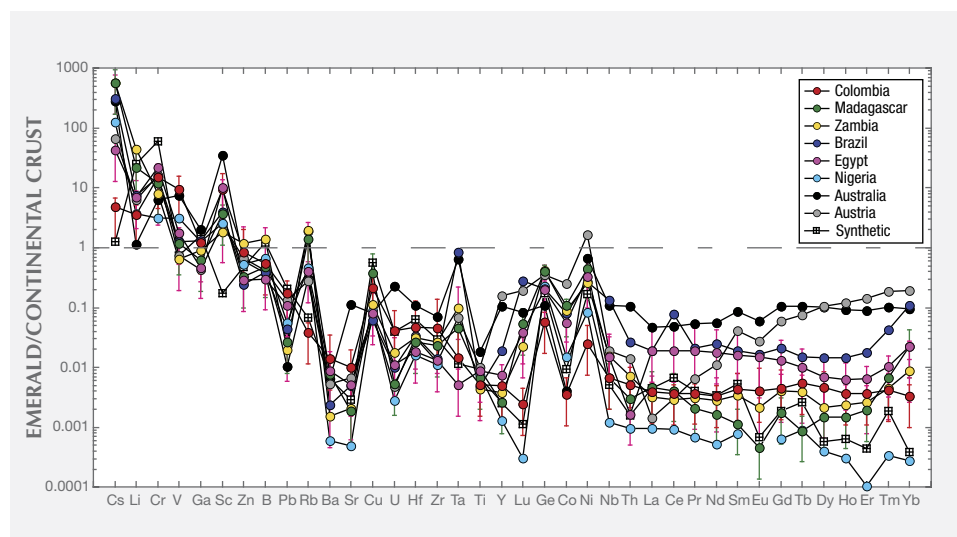


Figure 1. Multi-incompatible trace element plot normalized to bulk continental crust (Rudnick and Gao, 2004) for emeralds from Colombia, Madagascar, Zambia, Brazil, Egypt, Nigeria, Australia, and Austria, as well as synthetic emeralds.

The Proof of Provenance

Klemens Link

Gübelin Gem Lab, Lucerne, Switzerland

Consumers now demand more transparency on the provenance of the goods and services they purchase, an expectation that also applies to luxury products such as gemstones. Yet the gemstone trade has a reputation of being opaque. The Gübelin Gem Lab has kicked off a long-term initiative dedicated to closing this gap. Under the label Provenance Proof, technologies are developed that allow gemstones to be traced back to specific mines in order to provide more transparency throughout the chain of custody. The Provenance Proof initiative is independent of the traditional lab work, and all technologies are made available to the entire industry.

The first technology developed under the Provenance Proof initiative is referred to as the Emerald Paternity Test. The Gübelin Gem Lab has developed a physical tracer using nanolabels to suit the needs of the gemstone industry. These nanolabels are based on DNA fragments encapsulated in silica; with a diameter of 100 nm, they are invisible even to the most powerful optical micro-

scope. The identity of the mine and the miner, the exact location, the time period, and possibly further information are encoded into the DNA. The use of such labels allows the miner to tap the full potential of storytelling about specific provenance, including the possibility of independent proof of this source.

The nanotracers allow the tracing of a gemstone from the end consumer back to the original mine. Nevertheless, the other steps along the value chain remain nontransparent. To shed light on the entire value chain, we developed a digital logbook that allows the user to document all steps and transactions linked to a particular gemstone on its way from the mine to the end consumer. The backbone of this logbook is a hyperledger-based, community-controlled blockchain that is open to the entire industry and accessible with a smartphone. All data is securely encrypted and decentralized and only available to the holder or custodian of a specific gemstone.

General Gemology and Jewelry

Gemstones and Sustainable Livelihoods: From Mines to Markets



Saleem H. Ali

Gemstones and Sustainable Development Knowledge Hub, University of Delaware, Newark

Colored gemstone supply chains are highly fragmented. The large variety of gemstones found in the trade, each with different mining and manufacturing issues and production cycles, adds to this complexity. Yet this fragmentation also creates opportunities for diffuse positive impacts in livelihood formation across the supply chain. Gemstones are predominantly mined through artisanal and small-scale mining (ASM) operations, and many of those who mine the stones remain in poverty. Furthermore, the mining is often undertaken without any mechanism for environmental remediation that can sustain livelihoods beyond the mining phase. In a sector that ranges over 50 producing countries, with a multitude of cultures, environments, and minerals, much research remains to be done on how sustainability can be improved and catalyzed between mines and markets. The benefits that could flow from the sale and beneficiation of colored gemstones remain elusive and often accrue in favor of corrupt interests that could also exacerbate security concerns in fragile states. This sector is a neglected area for research and training and has also largely eluded international mechanisms for accountability such as the United Nations–mandated Kimberley Process for diamonds.

The gemstone industry can play a vital role in sustaining livelihoods and national economies following the cessation of mining. Thailand, formerly a gemstone mining nation, has succeeded in transforming its industrial sector to become the major international hub for the processing (treatment, cutting, and polishing) and trading of gemstones within a few decades. Thailand had a long tradition in gemstone manufacturing and has successfully moved up the gemstone supply chain. The country has achieved this transformation by transmitting know-how, fostering innovation in gemstone refinement, and embodying proactive governance structures. Case lessons like these must be understood and adapted to other geographies as far as realistically possible. The beneficiation of gemstones in their country of origin is a great challenge facing countries across the globe, but especially in Africa. Despite the value and the beauty of the stones, those who mine them and those in the first steps of the value chain often live in poverty. There are encouraging developments—for example, Tanzania has successfully created a gemstone cutting and jewelry-making hub, and the Ethiopian opal sector has had some promising developments in cutting and polishing.

Thus, from mines to markets, colored gemstones provide important opportunities for contributing to development and thereby improving the brand and value of the sector for consumers. However, an integrated mechanism for linking business imperatives with social development dimensions of the sector is essential. This pres-

entation will summarize some of the key research lessons gleaned through the Gemstones and Sustainable Development Knowledge Hub established in 2017 and the nascent educational program that is being developed through a network of international university partners on “Minerals, Materials and Society.”

Challenges of a Twenty-First Century Gem Trader

Edward Boehm

RareSource, Chattanooga, Tennessee

The gem trade looks much different than it did at the end of the last century. Previously the focus was on disclosure of synthetics and treatments, but in the last two decades it has evolved to include greater concern for sustainability, environmental conservation, and transparency in ethical sourcing. Country of origin has always played an important role in high-end gems, and this trend continues today, but the added element of traceability is changing the impact and importance of third-party verification. The country-of-origin pedigree associated with fine-quality gems from sources such as Myanmar (figure 1) and Kashmir has historically translated into desirability and higher value. However, today’s concerned consumer views a

country mired in sociopolitical conflict, war, genocide, or terrorism as an undesirable source, potentially leading to boycott by not only consumers but also NGOs and large or publicly traded jewelry companies. These challenges, while daunting, should also be viewed as opportunities for the entire gem trade.

Reputable gem dealers focus on finding quality gems sourced from reliable producers while competing for the best prices. Ethical sourcing is a main focus for many dealers, but recent sustainability and transparency requirements from larger retail chains are adding layers of responsibility that gem traders and gem trade organizations are working diligently to address. The American Gem Trade Association (AGTA), the International Colored Gemstone Association (ICA), and the World Jewellery Confederation (CIBJO) have been leaders in clear communication and disclosure to the consumer. Despite the demands of additional transparency, they face these challenges as opportunities to differentiate themselves by addressing the issues with positive and active policies. Membership in one of these organizations focused on ethical sourcing provides trade professionals with identifiable goals and guidelines to adhere to.

Modern tools to help gem traders adapt to these principles are becoming more available as demand increases. Professionals no longer have to rely only on their own gemological knowledge and contacts. Laboratory reports and now nanotechnology and blockchain tracking all provide potential third-party options for identifying and tracing the flow of gem material. Gemological laboratory reports and recent technological breakthroughs provide avenues for addressing some of the issues facing the trade, but they are not foolproof panaceas for the issues at hand. It will also take active good faith initiatives that involve the entire supply chain, from miners to retailers. As these technologies evolve and others are discovered, the trade will have even more ways to provide accurate information and confidence to consumers.

Figure 1. A gem miner holds a traditional brass plate of corundum, spinel, and peridot rough and crystals from Mogok, Myanmar. Photo by Edward Boehm.



San Diego Gemstones and Gem Localities

William Larson

Pala International, Fallbrook, California

For over 125 years, San Diego County has produced famous gemstone treasures. This talk will explore the history and famous localities from the original finds of the nineteenth century, as well as the connection to Chinese Empress Dowager Cixi (1835–1908). Her enthusiasm for San Diego gems led to an estimated 90 tons of tourmaline shipped to China before 1910 and the “type” locality finds of kunzite (figure 1) and morganite.

Of special interest, this presentation will detail the revival of San Diego gem mining starting in the 1950s and continuing to this day by looking at the three most important districts: Ramona for spessartine garnet and topaz; Mesa Grande for tourmaline; and Pala for tourmaline, morganite, and kunzite.

The author has been directly involved with 16 gem mining projects in San Diego County since the 1960s and has locally mined 36,000 feet of underground tunnel, resulting in many successful finds. The talk will also delve into current and future challenges for gem mining in San Diego County and elsewhere, including high mining costs—involving governmental, environmental, and safety regulations—and land-use restrictions. Possible bright spots for future gem mining localities include geophysical exploration techniques and underground radar, new mining techniques, and advances in explosives.

Figure 1. This 40.34 ct pink-lavender kunzite is from Pala, California. Photo by Mia Dixon/Pala International.



GIA's Field Gemology Program: A Modern Approach to Origin Determination

Wim Vertriest

GIA, Bangkok

Nowadays, origin determination is an undeniable part of gemology. For many high-end colored gemstones, country of origin is considered an important aspect that can significantly influence price. GIA realized early on that delivering trustworthy scientific studies on gemstone origin is a complex affair. It requires advanced technology, well-trained scientists, years of experience, and above all dependable reference samples.

Since the establishment of its field gemology department in 2008, GIA has built and maintained a reliable reference collection. The best way to collect samples is to cut out all intermediaries, thus removing any misinformation, and visit the mining areas in person to collect gemstones at the source, or as close to it as possible. GIA gemologists have observed and documented many of the most important ruby, sapphire, and emerald mining areas over the last decade (figure 1). Over 90 expeditions, over

20,000 reference samples—more than one million carats—have been collected.

The samples collected are integrated into GIA's colored stone reference collection. Each sample is accompanied by information detailing its sourcing, such as collection date, gem species, known treatment, previous owner details, GPS coordinates of mining and/or buying locations, and purchase price. All the data is subsequently available in an internal database that is accessible to GIA gemologists globally. When data (e.g., inclusion photos, trace element chemistry, and spectra) are collected on the samples, they are added to the database. This becomes an important resource to GIA colored stone gemologists in every location. In a video on scientific research collections, Sir David Attenborough noted:

a research library associated with collections is almost of greater importance than the objects themselves. Unless you know where it came

from *exactly*, and when it came from *exactly*, you are missing a lot of very, *very* important information. That information can not only come from the object itself, but from the circumstances, documentation, that should accompany every scientifically collected specimen. (“Sir David Attenborough on Museum Collections - 360,” American Museum of Natural History, posted August 31, 2017)

While in the field, GIA team members also document the local situation. This covers mining techniques, trading activity, traditional jewelry making, gemstone history, and local gem cutting. Videos, photos, and interviews are then used to create articles and supplement course content for GIA’s educational programs. In this way, the information gathered during field expeditions becomes an invaluable resource to multiple departments within GIA and serves as a historical record of gem mining sites around the globe.

Figure 1. Greenland ruby samples in matrix collected for GIA’s field gemology program. Photo by Wim Vertriest.



Closing the Knowledge Gap Across the Supply Chain: A Case Study of GIA and Pact’s Field Collaboration in Tanzania

Cristina Villegas

Mines to Markets Program, Pact, Washington, DC

For years, field gemologists and international development experts across disciplines have noted that colored stone supply chains are lopsided in terms of stakeholder knowledge about stone types, quality and grading, handling know-how, and what happens after the stone leaves the mine and its journey begins in the global jewelry supply chain. Those who mine the stones—typically at great personal risk—are usually the most likely to know the least about them. One stone can change a life if it is of especially high quality, while others may be “tourist grade” (local parlance for lower-value stones). Many artisanal and small-scale miners (ASM) simply do not realize the difference.

In 2017, the Gemological Institute of America and Pact, an international nonprofit social development organization with a specialty in developing and delivering ASM economic and social programs, joined forces to test a simple idea: Can a simple guidebook make a difference, and how?

The project, originally conceived by GIA distinguished research fellow Dr. James Shigley, is part of the Institute’s mission-driven effort to share information and skills throughout the gem

Figure 1. Miriam S. Mshana, an artisanal sapphire miner, is chairwoman of the Tanga chapter of the Tanzanian Women Miners Association (TAWOMA), a field partner that facilitated access to the remote mining sites. TAWOMA comprises more than 3,000 women working across the mining sector producing gold, colored gemstones, diamonds, and industrial materials. The Tanga chapter alone has 600 members. Photo by Cristina Villegas.



and jewelry industry supply chain and with the public. An area in Tanzania's Umba Valley was identified, and the program rolled out in 2017 with the Tanga chapter of the Tanzania Women Miners Association (TAWOMA; figure 1). The results were fascinating and validated the need for the guidebook. Of particular note: For every \$1 the project invested in artisanal and small-scale miners, there was a \$12 social return on the investment. Both male and female miners commented that they believe these changes they have experienced will last for more than five years.

This presentation will focus on how the project was implemented, monitored, and measured, and will engage the audience to help identify answers to these questions:

- How can the gemological research sector, and other parts of the jewelry supply chain, help advance local economic and social development agendas in sub-Saharan Africa?
- What other knowledge could be imparted in a context of low literacy? Are there other ways that learning programs could be structured to maximize impact in a given province? In other words, how can we improve in the future and also inspire others to act?

In reporting on her June 2018 trip to the region, the author will provide an update on the 2017 project participants.

New Technologies and Techniques

Synthetic CVD Diamond—30 Years On

Daniel J. Twitchen

Element Six, Global Innovation Centre, Harwell, Oxford, United Kingdom

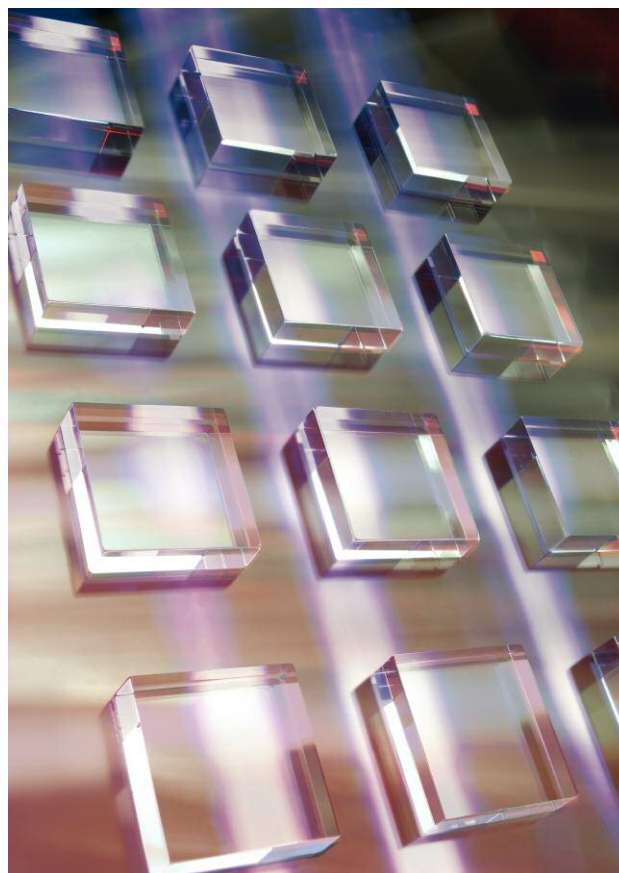
Element Six first started its chemical vapor deposition (CVD) synthetic diamond program in 1988. Thirty years on, this talk will review notable high and low points, flagging some lessons learned.

Volume synthesis of diamond by CVD (figure 1) has not only contributed to reducing the cost of the material but also enabled the superlative properties of diamond to be more fully utilized. It has long been recognized that, aside from its extreme hardness, diamond is a remarkable material with many properties—optical, thermal, electrochemical, chemical, and electronic—that outclass competing materials. When combined, these properties offer the designer an engineering material with tremendous potential to create solutions that can shift performance to new levels or enable completely new approaches to challenging problems.

Components routinely fabricated using CVD synthetic diamond now span tweeters for loudspeakers, radiation detectors and sensors, optical components for lasers, windows for radio frequency and microwave transmission, blades and cutting tools, and electrodes for electrochemical sensing, ozone generation, and direct oxidation of organic matter.

Lightbox, a new De Beers company, has recently announced jewelry using white, blue, and pink lab-grown CVD diamonds. As crystal growers and materials scientists know, intrinsic undoped diamond is colorless in the visible range, but its absorption properties can be modified by defects, often referred to as “color centers,” formed either during the CVD growth process or through post-growth treatments such as irradiation and annealing. This presentation briefly summarizes some of the tools used to engineer CVD diamond. For example, controlling the nitrogen level (yellow CVD) to obtain particular thermal and optical properties,

Figure 1. Single-crystal CVD diamond. Courtesy of Element Six.



doping with boron (blue) to make electrically conducting diamond used to produce ozone for sanitization and for thermal management in telecommunications, and growing in nitrogen-vacancy centers (pink) to make magnetic sensors.

The diverse applications of diamond that harness its exceptional properties and the impact of color centers touch our lives in unexpected ways: Diamond is used to create the high-quality mirror finish on your smartphone and to produce the 170 miles of copper wiring in the aircraft that takes you on vacation, and it

is also enables new higher-power lasers used in welding our cars together. It is even used in the quality control of food and in pharmaceutical manufacturing.

In summary, there has been considerable progress in the fabrication and commercialization of CVD-grown diamond over the last 10 years by a number of producers. This progress, coupled with the broad range of applications, shows that perhaps a new age of industrial diamond has truly begun—the age of CVD synthetic diamond.

Beyond Gemstones: The Medical, Industrial, Scientific, and Computational Applications of Lab Diamonds

Jason Payne

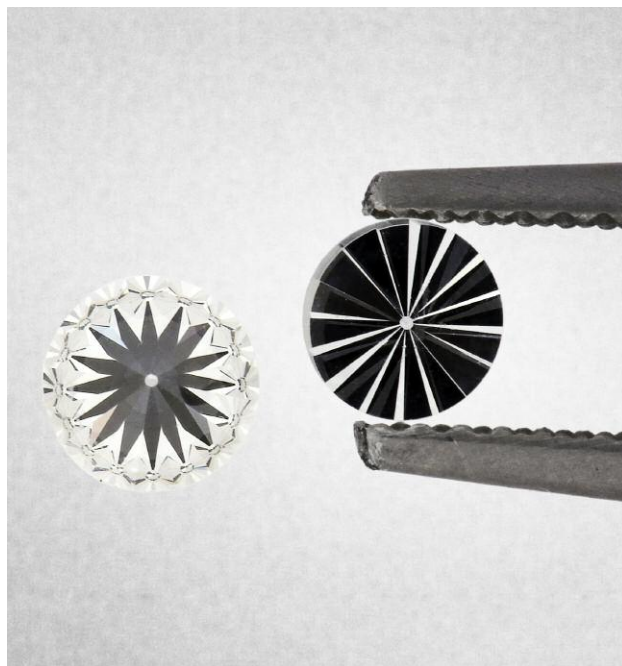
Ada Diamonds, San Francisco

Many gemologists know that there are important technological applications for laboratory-grown diamonds; however, it is less understood how broad the nongemological uses really are or why diamond is the ideal material for each use. This presentation will review modern industrial applications of laboratory-grown diamonds, including surgical tools, tumor detection, orthopedic implants, water purification, industrial tooling, compound refractive energy focusing, Fresnel lenses, high-pressure anvils (figure 1), sound reproduction, deep space communication, high-power electronics, quantum computing, long-term data storage, AC/DC conversion, and electrical vehicle efficiency.

These applications are rooted in the less frequently discussed gemological properties of diamonds that make it a “supermaterial.” The biological, thermal, mechanical, optical, acoustic, and electrochemical properties of diamond will be introduced. Specific properties discussed will include thermal conductivity, Young’s modulus, breakdown field, band gap, and saturated electron drift velocity. Furthermore, the utility of diamond defects such as nitrogen vacancies and boron will be explored.

In addition to discussions about functional monocrystal diamonds, two unnatural forms of functional diamond will be discussed: polycrystalline diamond (PCD) and diamond-like carbon (DLC). Many of the functional diamonds discussed, including PCD and DLC, will be available for hands-on examination as part of the presentation.

Figure 1. Laboratory-grown diamond anvils, capable of generating 1 terapascal of pressure, enable high-pressure experiments for physics, chemistry, materials science, and industry. Photo courtesy of New Diamond Technology.



Big-Data Analysis and Insights in the Online Gem and Jewelry Trade

Menahem Sevdermish and Guy Borenstein
Gemewizard, Ramat Gan, Israel

Big-data analytics is the process of collecting, organizing, and analyzing large volumes of data to reveal hidden patterns and unfamiliar correlations, identify market trends, and extract other useful information that might otherwise be invisible—even for the data manager.

Big-data analytics is seldom used within the gem and jewelry trade. The gem and jewelry sector is kept with general fixed inquiries that block the category from characterizing its inventory and users, and by that, identifying new opportunities.

Another challenge is that in most online marketplaces, the “What You See Is What You Get” experience is hindered by two main factors: improper disclosure and misrepresentation of images (e.g., digitally enhanced photos).

The research and development team of Gemewizard has devised and digitized a fully automatic big-data analysis system for large-scale gem and jewelry marketplaces, based on color and contextual search engine and image analysis (figure 1). This system generates unique market analytics and a fraud detection and prevention service.

Since 2016, the Gemewizard team has had the opportunity to examine the validity of the system using vast amounts of data from a world-leading online retail marketplace. The information gathered from this survey, together with additional volumes of information collected from the Internet, provided some important insights regarding the online gem and jewelry trade. Some of these insights, which we consider fruitful and eye-opening for any marketplace or e-tailer, will be revealed.

The gem-related information contains insights regarding common fraudulent activities and practices for 128 varieties, species, and series of merchandisable gems. The gathered data includes anomalies in attributes such as:

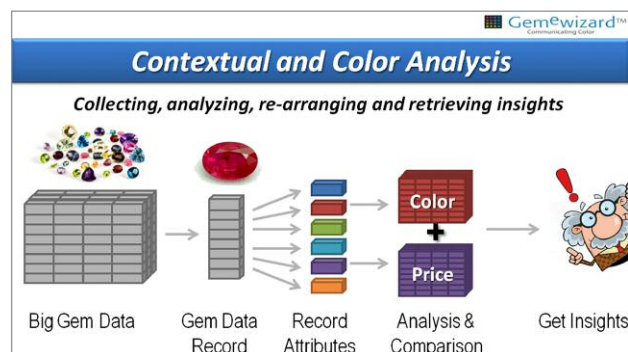
- Gem type: Mineralogical, gemological, and trade names, as well as misnomers. Analysis includes accepted word

combinations (e.g., “ruby” and “zoisite”) versus problematic ones (e.g., “diamond” and “moissanite”).

- Color (e.g., “yellow emerald”)
- Synthetic wording and nicknames (e.g., “heating with light elements”)
- Treatment wording, ranked and analyzed according to severity (e.g., “heating” versus “diffusion” in ruby)

The trade-related information provides powerful forecasting tools for the marketplace administrator. These include sales and trends history, defined by attributes such as type, color, geography, seasonality, and price, and the ability to identify tendencies (e.g., “Prices of untreated ruby gems between 2 and 3 carats are on the rise in Europe...”) and pricing opportunities (e.g., “Currently, there is a high demand for pale-colored Paraíba tourmaline gems in Far East markets”).

Figure 1. The system algorithm crawls the HTML pages of gem websites for big data. For each gem, it condenses the item page to its attribute components and records useful data. The collected data is then compared against the entire database to identify insights and peculiarities.



Diamond Impression: The Key to Sustainable Competitiveness

Sergey Sivovolenko¹, Roman Serov², and Janak Mistry³ (presenter)

¹OctoNus Finland Oy, Tampere, Finland

²OctoNus Software, Moscow

³Lexus SoftMac, Surat, India

People are impressed with the uniqueness of diamond, which incorporates factors such as brilliance and fire. When the trade commoditized the category through the Four Cs, it was partly due to

the technical inability to promote diamond’s impressive optical effects, including optical illusions. This common trade practice inhibited diamond’s competitiveness against other goods in the

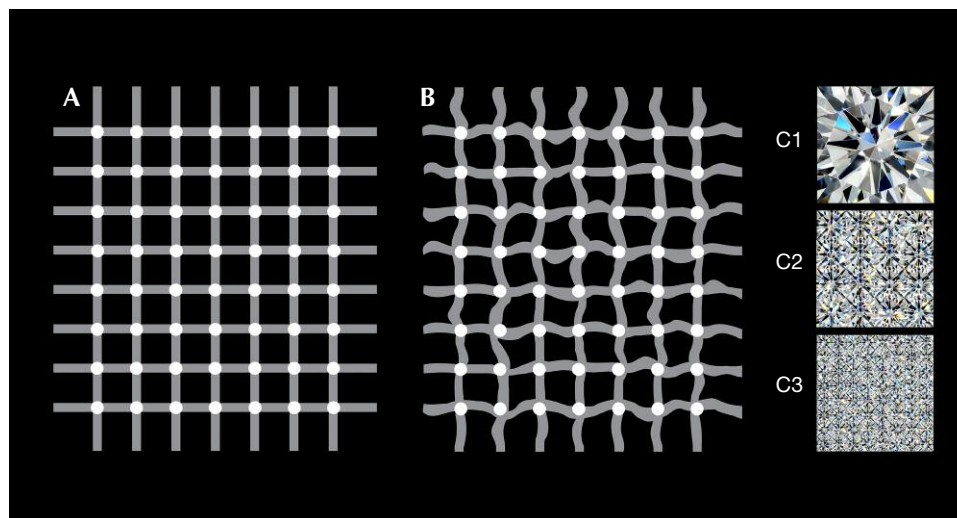


Figure 1. A scintillation grid (A), a scintillation grid with a wavy pattern (B), and squares covered by round brilliant-cut diamonds in different sizes (C).

luxury sector. But from now on, emerging technology will allow demonstration of diamond's magic on a large scale with fine details.

Modern algorithmic craftsmanship creates the category of high-vibrancy diamonds, referred to here as Hi-Vi: exceptional diamonds with superior consumer benefits such as brilliance, fire, table color, symmetry, and spread, compared to others of the same shape, size, and pavilion color. The triple excellent round, which took centuries for the industry to craft, was the first Hi-Vi diamond.

Diamond vibrancy is a combination of optical effects and illusions. For example, brilliance, fire, scintillation, and spread depend on both objective parameters such as cut design and stone size, as well as subjective aspects of human vision, such as space-temporal sensitivity and stereo perception. Figure 1A demonstrates the scintillating grid illusion: The intersections seem to flicker white and black, generating additional brightness and contrast when the observer's glance wanders. Distortion of pattern ruins this effect (figure 1B). Certain patterns produce higher perceived brightness. This example is a 2D effect; more astonishing optical illusions result from human stereo vision.

The phenomenon of diamond brilliance has a similar origin—human vision peculiarity—as the scintillating grid illusion

described above. The impact of optical illusions on both Hi-Vi diamond patterns and jewelry designs (e.g., melee) are to be considered, so Hi-Vi optimization is made for not just single diamond cuts, but also for each diamond jewelry piece as a whole.

Figure 1C shows squares with round brilliant-cut (RBC) patterns that differ only in size. The integral colored and colorless areas are exactly the same, while the perceptions of fire and brilliance in each image are quite different. It is impossible to maximize two performance parameters (both fire and brilliance, for example) simultaneously. The consumer's final choice should be based on subjective preferences and rely on performance benchmarks.

Hi-Vi diamonds should be demonstrated with an optical performance digital “loupe,” which allows even inexperienced buyers to easily appreciate the performance difference at the highest levels of brilliance, fire, and scintillation. The “loupe” is critically important for mass marketing of relatively small diamonds. For sustainable market development, diamond impressiveness and vibrancy born of masterly designed optical illusions and visual effects is the selling proposition to craft, demonstrate, and explain.

For online access to all issues of GEMS & GEMOLOGY from 1934 to the present, visit:

gia.edu/gems-gemology

